CHARACTERIZATION OF SOCIAL STATUS-DEPENDENT NEUROMODULATION IN ZEBRAFISH (*DANIO RERIO*)

by

Thomas H. Miller

June, 2017

Director of Thesis: Dr. Fadi A. Issa, Ph.D.

Major Department: Biology

In zebrafish (*Danio rerio*), social interactions between adult males consist of a series of aggressive encounters that ultimately lead to the formation of stable hierarchies of either socially dominant or subordinate animals. Although it has been shown that social status leads to neurophysiological changes in brain structure and function, our understanding of the underlying mechanisms that control behavioral function remains limited. We show that socially dominant animals display increased swimming activity. Conversely, social Subordinates display decreased swimming activity, but an enhanced sensitivity of the C-start escape circuit. We also show that whole brain expression of dopamine transporter (DAT) was significantly up-regulated in Dominants compared to Subordinates. In addition, Dopamine 1 receptor (D1R) expression was down-regulated in Subordinates compared to Dominants, suggesting that there is a social-status dependent regulation of the dopaminergic (DA) system. Finally, we show that visual cues play an important role in regulating zebrafish dominance relationships and the prioritization of different motor outputs by using a zebrafish line lacking pigmentation. Taken together, our results reveal that neuromodulation by DA signaling and visual information provides a mechanism for the nervous system to adapt to changes in social conditions by permitting the animal to prioritize a socially appropriate behavioral response.

CHARACTERIZATION OF SOCIAL STATUS-DEPENDENT NEUROMODULATION IN ZEBRAFISH (*DANIO RERIO*)

A Thesis

Presented to the Faculty of the Department of Biology

East Carolina University

In Partial Fulfillment of the Requirements for the Degree

Master of Science in Molecular Biology and Biotechnology

by

Thomas H. Miller

June, 2017

CHARACTERIZATION OF SOCIAL STATUS-DEPENDENT NEUROMODULATION IN ZEBRAFISH (*DANIO RERIO*)

by

Thomas H. Miller

APPROVED BY:

DIRECTOR OF
THESIS: _____
Fadi Issa, PhD

COMMITTEE MEMBER: _____
Stefan Clemens, PhD

COMMITTEE MEMBER: _____
Ed Stellwag, PhD

COMMITTEE MEMBER: _____
Yong Zhu, PhD

CHAIR OF THE DEPARTMENT
OF BIOLOGY _____
Jeff McKinnon, PhD

DEAN OF THE
GRADUATE SCHOOL: _____
Paul J. Gemperline, PhD

TABLE OF CONTENTS

LIST OF TABLES

LIST OF FIGURES

LIST OF ABBREVIATIONS

5-HT	Serotonin
COMT	catechol-O-methyltransferase
CPG	Central pattern generator
cx41.8	connexin 41.8
DA	Dopamine
DAT	Dopamine transporter
DCC	L-Dopa decarboxylase
D1R	Dopamine 1 Receptor
D2aR	Dopamine 2a receptor
D2bR	Dopamine 2b receptor
D3R	Dopamine 3 receptor
i-IN	inhibitory interneuron
M-Cell	Mauthner Command Neuron
MAO	monoamine oxidase
MN	motor neuron
mitfa	microphthalmia-associated transcription factor a
MLR	mesencephalic locomotor region
nMLF	medial longitudinal fasciculus
POA	preoptic area
SDM	social decision-making network
TH	tyrosine hydroxylase
TLN	Tupfel long fin nacre
VIIIth Nerve	vestibulocochlear sensory nerve

VMAT	vesicular monoamine transporter
VTA	ventral tegmental area
WHO	World Health Organization

CHAPTER 1

GENERAL INTRODUCTION

Aggressive interactions are something that we as a species deal with every day. In 2002, the World Health Organization (WHO) released a comprehensive review of violence and aggression and their effect on health; and define aggression as "the intentional use of physical force or power, threatened or actual, against oneself, another person, or against a group or community, which either results in or has high likelihood of resulting in injury, death, psychological harm, maldevelopment or deprivation" [32]. Importantly, not only does the WHO definition highlight the physical component of violence, but also the downstream effect that aggression may have on the individuals involved. These effects may be readily apparent as physical harm but there are often unseen effects on a neurological level that may be more harmful in the long-term. Repeated aggressive acts, or chronic social stress, have been linked to the development of psychosis [43], depression, anxiety, and increased risk for psychiatric disorders and suicidal thoughts [62]. By understanding how long-term social-stress impacts the nervous system, we would be able to develop more tools for the mitigation and treatment of these disorders. Human motivation can be tricky to fully understand, but motivations behind aggression can be distilled down to the desire to achieve some benefit for the aggressor at the expense of another. Therefore, the aggressors seek to increase their fitness in some way. While humans are unique in their displays and methods of aggression the neural mechanisms that drive aggressive behavior are likely conserved across social species [47, 48]. Therefore, studying social aggression in non-human animals may give us mechanistic insights into the neural bases of aggression and possible targets for the treatment of its negative effects.

Zebrafish as a Model for Social Aggression

Intraspecific social interactions are inherent to any social animal. Competition for limited resources such as food, territory, reproductive success, and social rank leads to the formation of dominance hierarchies; ultimately facilitating group organization and stability [35, 52, 72]. Competition causes group members to prioritize some behaviors over others depending on their social rank. This choice of behavioral output is consolidated by the integration of social cues. The neural bases of behavioral choice and adaptation to changing social dynamics have been investigated in invertebrate and vertebrate animals [6, 17, 46, 71, 77]. However, the long-term effects of social status on nervous system function are poorly understood [15, 43]. Having a model system that displays robust aggressive social behavior that can be probed neurophysiologically and molecularly is critical in identifying underlying mechanisms of how social factors can exert physiological changes in brain function.

Zebrafish (*Danio rerio*) are a growing neurobiological model for the study of vertebrate behavior [9], social stress [17], major depressive disorders [39], and aggression [35, 50, 52]. Zebrafish are a highly social species, live in large communities and exhibit social preference for conspecifics by schooling [4]. Within these schools, zebrafish do exhibit territoriality and aggressive behaviors, although these acts of aggression are more subtle and less frequent compared to dyadic interactions [4, 35]. However, social behavior of zebrafish can be manipulated based on the number of fish within a community [37], and pairs of zebrafish have been shown to elicit robust aggressive behaviors that are readily observable [35, 67]. It is important to note that dyadic interactions among zebrafish males do not typically occur naturally, so aggressive interactions between male pairs may not be an accurate representation of social behavior in zebrafish communities. However, paired zebrafish offer a robust model for the study

of aggressive interactions and may provide insights into the effects of aggression in other vertebrate systems. Dyadic interactions of zebrafish lead to the development of dominant and subordinate individuals. Typical behaviors elicited in a social context are aggressive chasing and biting (attacking) performed by Dominants, or retreating elicited by the Subordinates [35, 50]. The primary focus of the investigation into zebrafish social interactions has been in the initial establishment of the social dominance, typically within a week of pairing [9, 35, 50, 52]. However, zebrafish form stable social hierarchies that are long lasting (>1 month), making them a useful model to study the long-term effects of chronic social aggression on brain function.

Although little is known of about how the nervous system adapts to chronic social stress, potential modulators include dopamine (DA), serotonin (5-HT), and Vasopressin [35] have been implicated in playing a role in regulating aggression, motivation and depression [9, 16]. However, these neurochemicals are widespread, and unevenly distributed throughout the central nervous system; determining the mechanisms behind how they may change underlying neural circuits' activity is challenging. As a first step, here we investigated how social status regulates the activity and signaling of DA and how differential regulation may account for differences in the activation of motor networks.

Thesis Outline

In this study, we investigated the effects of social experience and social rank on the behavioral outputs of adult male zebrafish. Toward this end, we examined the effects of social status on two well-studied behaviors: swimming and the Mauthner neuron-mediated escape response. The functional and anatomical organization of the underlying neural circuits mediating these two behaviors is well characterized morphologically and functionally [1, 11, 27, 51, 66, 55, 78, 65].

Using conventional behavioral observation and non-invasive electrophysiology techniques, we were able to determine that these two motor outputs are modulated based on the social rank of the animal. These results will be discussed in detail in Chapter II. We then used a neurocomputational model and gene expression analysis to investigate potential mechanisms behind the modulation of the swimming and escape behaviors. We investigated two sources of neuromodulation within the zebrafish brain: DA and visual information by the way of social cues.

Chapter II will highlight neuromodulation by DA, particularly how the expression of select genes in the DA pathway is altered by social status. Chapter III will then explore the role of visual cues in a social context by presenting data collected from zebrafish lacking pigmentation. Our data provides evidence that visual information plays a vital role in the normal formation of a social dominance in zebrafish and that DA may be important for social status-dependent modulation of motor outputs.

CHAPTER II

SOCIAL STATUS MEDIATED CHANGE IN BEHAVIOR VIA DOPAMINE

Previously Published:

Miller, T.H.*, Clements, K.*, Ahn, S., Park, C., Ji, E.H., Issa F. Social status-dependent shift in neural circuit activation affects decision-making. Journal of Neuroscience. 22 February 2017, 37 (8) 2.137-2148

*Equal first authorship. Both authors contributed equally to this work.

INTRODUCTION

To investigate the effects of social stress on nervous system function, we examined the implications of social status on two well-studied behaviors: swimming and the Mauthner neuron (M-cell)-mediated escape response. The functional and anatomical organization of the underlying neural circuits mediating these two behaviors is well characterized morphologically and functionally [1, 11, 27, 51, 66, 69, 78, 80]. The C-start escape behavior is mediated by the Mauthner Command neurons [34, 78]. The Mauthner neurons are a pair of interneurons in the hindbrain that receives auditory and tactile input and sends projections across the midline to innervate spinal cord motor neurons contralaterally. Therefore, unilateral activation of the Mauthner allows the fish to flex in the characteristic C-bend and escape away from the stimulus by activating the fast flexor muscles (Figure 1) [51, 78]. The morphological and electrophysiological properties of the M-cells, as well as the circuitry of the C-start escape behavior, have been well characterized [1, 11, 12, 30, 33, 51]. The Mauthner neurons receive ipsilateral inputs from the ear via the vestibulocochlear sensory nerve (VIIIth cranial nerve).

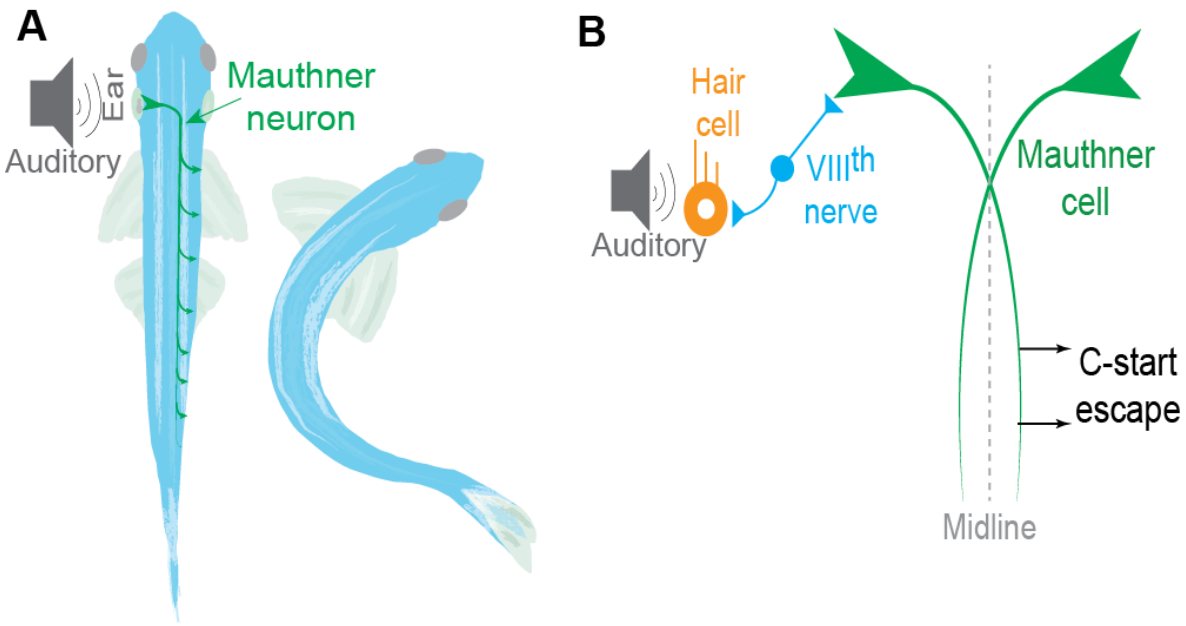

Figure 1 - Schematic illustrations of the M-cell escape circuit
A) Zebrafish startle response is activated by auditory stimuli. C-start behavior is mediated by the well-characterized Mauthner neural circuit. Activation of the M-cell is necessary for c-start escape. M-cell innervates spinal cord motor neurons. B) Schematic illustration of the M-cell escape circuit. M-cell escape response is initiated via activation of the VIIIth sensory nerve

The synapse of the VIIIth nerve with the M-cell contains both chemical components, via glutamatergic signaling, and an electrical component through desmosomes and gap junctions [42, 55, 56, 75]. Therefore, the Mauthner neurons can exert a rapid, high fidelity response upon stimulation by an auditory stimulus.

Neural circuitry underlying swimming is less centralized compared to the C-start escape circuit but is still under tight hierarchical control [66, 68, 70]. In zebrafish, the mesencephalic locomotor region (MLR) initiates swimming [5, 27] and sends projections to reticulospinal neurons in the hind- and midbrain. These interneurons then excite spinal central pattern generator nuclei (CPGs) to drive the oscillatory contraction of the slow flexor muscles needed for rhythmic swimming [10]. Interestingly, both the escape and swim circuits receive visual and postural sensory information from higher brain regions [29, 45, 57] and are regulated by neuromodulatory inputs [41, 55]. Therefore, these circuits and their associated behaviors may be susceptible to plastic changes wrought by an animal's relative social experience.

Here, we investigated how social rank affects the activation patterns of escape and swim behaviors. We accomplished this by behavioral observation and a non-invasive technique to monitor the patterns in freely behaving animals [23, 59]. We show that these neural circuits shift their activation depending on an animal's social status. In order to link the behavioral observation with putative cellular changes, we present a computational model illustrating how a change in the relative excitability of these circuits can facilitate the transition between the dominant and subordinate behavioral phenotypes.

Dopaminergic signaling and modulation

In addition to changes in behavioral output, social status is regulated by neuromodulators [55, 41]. Social interactions have been shown to change the expression of critical genes in hormone and neurotransmitter signaling such as DA and 5-HT during the establishment of a social hierarchy [16, 53]. While 5-HT may play an important role in social regulation within this system, we focused on DA for this study. Functionally, DA is a neurotransmitter involved in sensory-motor programming, motivation, memory, emotion, and endocrine regulations [74]. Given the sensorimotor nature of the swimming and Mauthner escape circuits, DA seems like a likely candidate to play a role in social status-dependent modulation of motor behaviors like swimming and the C-start escape.

DA is a monoamine derived from the amino acid tyrosine by the enzymes tyrosine hydroxylase (TH), and L-Dopa decarboxylase (DDC). Following its synthesis, DA is packaged into vesicles by the vesicular monoamine transporter (VMAT), ready to be released into the synapse following an action potential. Once in the synaptic cleft, DA can: 1) be reabsorbed back into the presynaptic cell or by surrounding glial cells via the dopamine active transporter (DAT) 2) be degraded by monoamine oxidase (MAO) and catechol-O-methyltransferase (COMT), or 3) bind to a DA receptor pre- or post-synaptically (Figure 2). DA receptors are divided into two classes, DA receptor 1 (D1)-like, and DA receptor 2 (D2)-like receptors. Both receptor subtypes are coupled to associated G-proteins and affect levels of cAMP, Ca^{2+} influx into the cell, as well as K^{+} flow. D1-like receptors (D1 and D5 receptor subtypes) interact with Gs and Gi proteins and increase the excitability of downstream neurons. D2-like receptors (D2, D3, and D4 receptor subtypes) are linked to Gi proteins and conversely decrease the excitability of downstream cells. D2-like receptors can also function as an autoreceptor on the presynaptic neuron in a negative

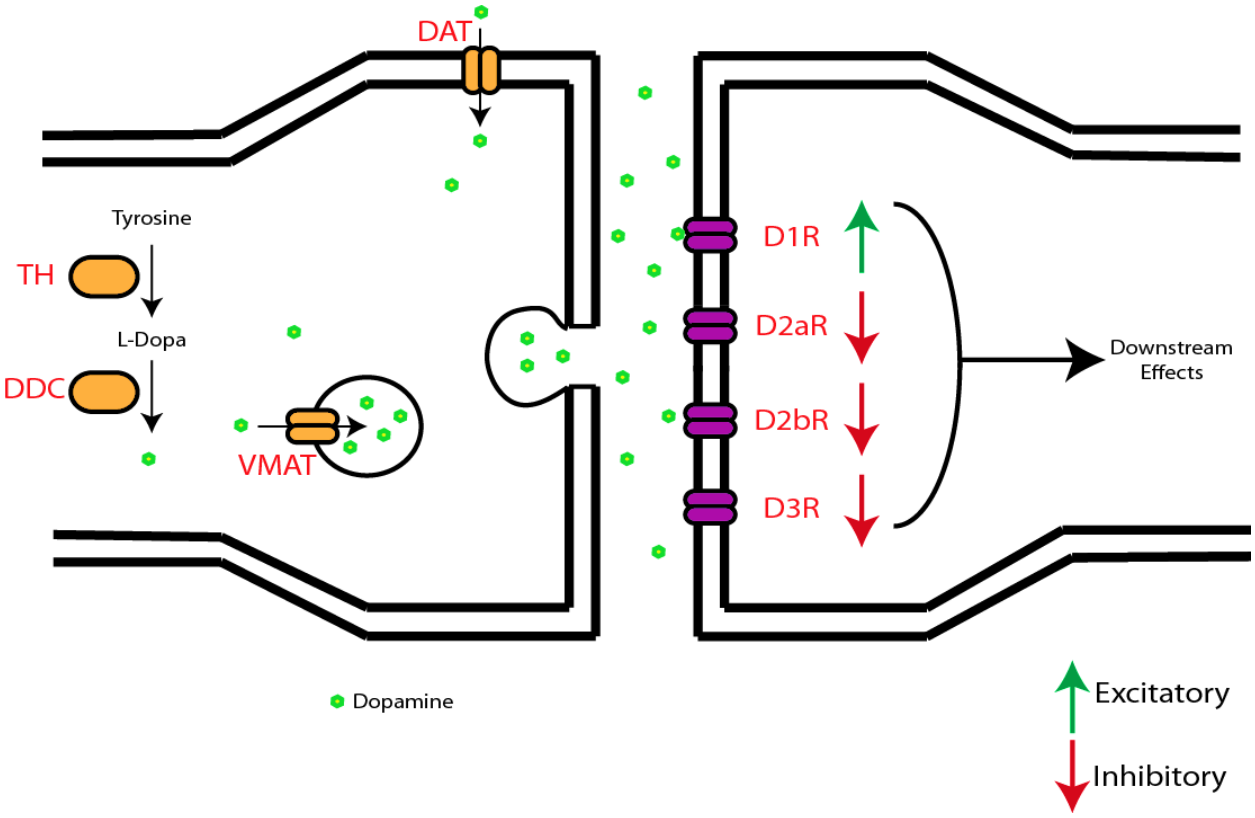

Figure 2 - Schematic of Dopaminergic Synapse

feedback mechanism.

Dopaminergic inputs have been identified near the electrochemical synapse of the Mauthner neurons and the VIIIth nerve, but have not been shown to form direct synaptic inputs [49]. Also, exposure of the Mauthner neurons to DA has been shown to modulate the sensitivity of the C-start escape and the efficacy of the electrochemical synapse in both a cAMP-dependent and independent manner [45, 54, 55, 76]. This evidence lends credence to DA having a modulatory effect on the Mauthner neural circuit. Previous reports have also shown that social status influences the expression of dopaminergic genes in zebrafish during the establishment of a social hierarchy [16, 53].

While the C-start escape has been shown to be DA responsive, the overall effect of DA exposure to the circuit ultimately depends on intrinsic properties of DA signaling on the M-cell circuit. Namely, changes in the expression of genes involved in the supply or interpretation of the DA signal could ultimately change the behavioral output of spinal motor circuits (swim and escape circuits). Therefore, we hypothesize that social experience alters the expression of DA-related genes differently in dominant vs. subordinate fish to prioritize certain behavioral outputs relevant to their social rank. To test this hypothesis, we examined the expression of eight genes involved in DA signaling on a whole brain and regional level to determine if they are socially regulated.

In an attempt to examine the potential neuromodulation of these circuits, we examined the expression of DA-related genes in whole brain tissue of dominant and subordinate animals. We found that Dominants and Subordinates show altered expression of DAT and D1 depending on their social rank.

EXPERIMENTAL METHODS

Animal care and use – Experiments were carried out following National Institutes of Health guidelines and East Carolina University's Institutional Animal Care and Use Committee approval. Adult strain AB zebrafish (*Danio rerio*) were maintained at 28 °C, pH 7.3, and fed in excess three times daily. Group-housed males were placed into isolation for one week and then paired for a two-week period until a stable social dominance is formed. In order to collect brain tissue samples isolated, dominant, and subordinate fish were euthanized by hypothermic shock on ice for 20 minutes. Dissections were performed in ice-cold sterile Hank's balanced salt solution to preserve sample integrity and prevent RNA degradation. Whole brain tissue was dissected, and placed into a sterile microcentrifuge tube. Whole brain samples were stored at -80 °C until use. Hindbrain and hypothalamic brain tissues were collected and placed into pre-weighed, sterile microcentrifuge tubes. Brain region samples were stored at -80 °C until they were processed.

Measuring swimming activity - Pairs of animals were filmed daily (early afternoons) for one minute to their swimming activity using a Canon Camcorder (Digital video ZR500). Videos were digitized, down sampled to 3 frames per second, and movement (distance traveled over one minute periods) of each fish was analyzed using NIH ImageJ software Manual Tracking plugin. Instances when animals were interacting with one another resulted in the exclusion of those video frames from analysis. Total tracked distance was normalized by the number of remaining video frames.

Place preference during pairing - The movement of the animals was tracked using the Manual Tracking plugin for ImageJ to extract XY coordinates within their housing tanks. Videos were down-sampled to 3 frames/second and coordinates for Dominants, and Subordinates were loaded into R software using a custom script. XY coordinates encompassing periods of social interactions were removed from the analysis. Filled contour plots combining data of all dominant or subordinate animals were produced using 2D kernel density estimations generated by the kde2d function of the MASS package (CRAN repository) [69]. The algorithm used disperses the mass of the empirical distribution function over a regular grid of 512 points and uses the fast Fourier transform to convolve this approximation with a discretized version of the kernel followed by linear approximation to evaluate the density at the specified points. Density data was converted into a heat-map probability plot to facilitate illustration of the data set for both social phenotypes.

Measurement of field potentials – Animals were placed in the testing chamber (Figure 3A) and allowed to acclimate for 30 minutes. Subsequently, field potentials of burst swimming activity were recorded continuously for 1 minute. Data acquisition, amplification, digitization and storage were the same as stated above. Swim bursts were detected and sorted using the "threshold" search tool of the Clampfit software (Molecular Devices). Detected bursts were processed and verified according to the following criteria: a burst was included if it was larger than 12 mV in total amplitude and had a 50-200 ms duration (Figure 3B). Markers were assigned to each burst at half-width of the burst (usually at the peak burst amplitude) for all bursts during the 60 second recording period.

Field potential data analysis - The latency of the escape response was measured using the field potential signals recorded by measuring the time between stimulus onset and beginning of field potential response. The zebrafish escape response is categorized into two main types of escapes. Activation of the M-cell generates a short-latency escape response with a time onset ranging between 5-15 ms (Figure 3B). Zebrafish also produce long-latency non-Mauthner mediated escapes with a time onset ranging between 15-40 ms [12]. Each type of escape generates a distinct electric field potential signal that permits the reliable identification of the type of escape based on the field potential signature and its latency from stimulus onset [23]. The latency of the electrical signal was defined as the time difference between the onset of the auditory stimulus and the beginning of the large phasic field potential generated during the short-latency M-cell mediated escape response. Data was tabulated into Microsoft Excel and analyzed using Prism (GraphPad software Inc., San Diego, USA). All values are provided as mean and ±SEM unless otherwise stated.

Neuronal Model - A simplified single-compartment conductance-based biophysical model of the escape and swim circuits of the zebrafish was developed based on experimental data (Figure 7A) [29, 30, 67]. The model assumes that the stimulus is directly delivered to the M-cells. Only M-cells are considered as the main command neurons, but other Mauthner homologs including MiD2 and MiD3 cells may also play an important role in the escape behavior [45]. An external stimulus excites one of two M-cells while its contralateral homolog is inhibited by inhibitory commissural neurons [25, 79]. The model incorporates two different motor neuron populations, fast and slow, which are not functionally overlapped [2, 3, 67]. Moreover, we assume that the fast motor neurons (Fast MNs) that drive the escape behavior are only activated when they are

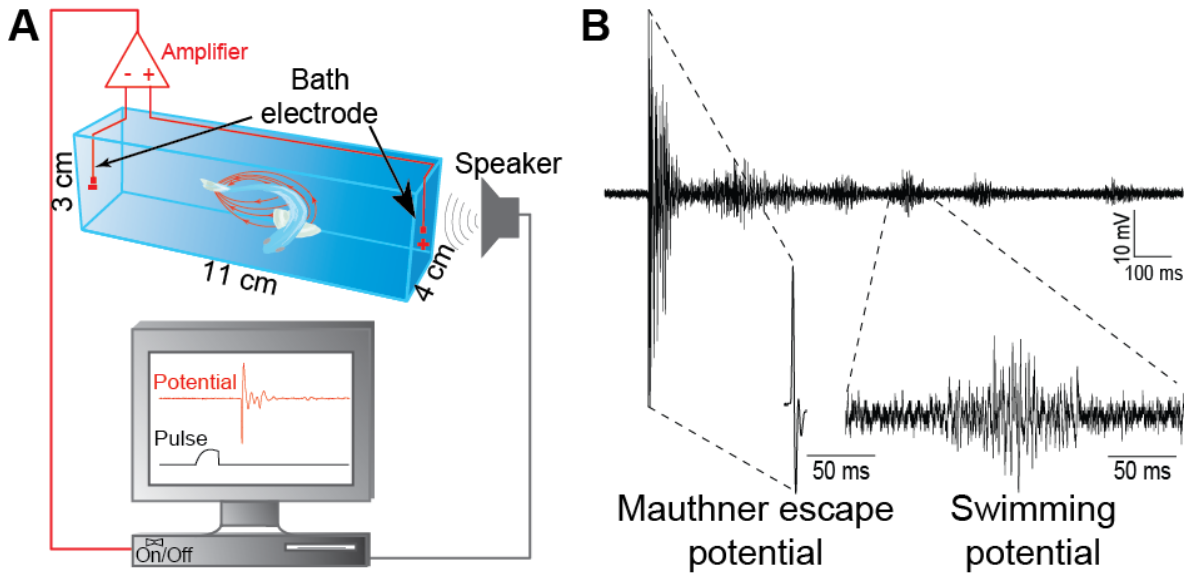

Figure 3 – Behavioral quantification by non-invasive electrophysiology
A) Schematic of testing and recording chamber used to measure C-start escapes and swimming activity. A pair of bath electrodes is placed on either side of the testing chamber. Bath electrodes detect neuromuscular field potentials generated as the M-cell escape response is activated. M-cell escape is activated by an auditory pulse. Field potentials and stimuli are time-locked and digitally recorded. B) An illustrative example of a phasic field potential recording recorded during activation of the C-start escape response mediated by the M-cell. This phasic response was followed by repeated swim bursts that were significantly lower in amplitude.

excited by the M-cells. On the other hand, the slow motor neurons (Slow MNs) receive excitatory inputs from the CPGs for swimming behavior and an inhibitory input from the inhibitory interneuron (i-IN), which receives excitatory inputs from the M-cells. Inhibition plays multiple roles in the generation of the activity patterns in the model. In particular, the reciprocal inhibition between CPGs is essential to generate alternate swimming patterns of Slow MNs, which is crucial in the normal swimming patterns of the zebrafish. The inhibition from the i-IN to the Slow MNs is also crucial to pause the swimming activity during the escape behavior and resumes with the termination of the escape. We assumed that the active M-cell directly inhibits its homolog, but this reciprocal inhibition is not essential in the simulation as long as M-cell cannot be active without an external input (see Figure 7A for a model network).

We consider the following simplified neuronal model for the escape and swimming behaviors of the zebrafish. To simulate the effect of an external stimulus on the M-cell, a depolarizing current pulse was applied to the M-cell model neuron. Stimulus activates the left M-cell, which results in the activation of right Fast MN in the contralateral sides while right M-cell is inhibited by the active left M-cell. The active M-cell also initiates the activation of i-IN, which results in the inhibition of all Slow MNs. A single model neuron represents the same set of neurons on each side.

We use conductance-based modified Morris-Lecar neuronal models [14, 24, 44] with additional calcium-dependent potassium in the following form:

Equation 1:

$$C\frac{dv}{dt} = -I_{Ca} - I_K - I_L - I_{KCa} - I_{syn} + I_{app}(t),$$

where $I_K = g_K n\,(v - v_K)$, $I_{Ca} = g_{Ca}\, m_\infty(v)(v - v_{Ca})$, $I_{KCa} = g_{KCa}\left\{\frac{[Ca]}{[Ca]+k_1}\right\}(v - v_K)$, $I_L = g_L(v - v_L)$ represent the potassium, calcium, calcium-dependent potassium, and leak currents. m_∞ is instantaneous voltage-dependent gating variable for the calcium current where

Equation 2:

$$m_\infty(v) = 0.5\left(1 + \tanh\left(\frac{v - v_1}{v_2}\right)\right).$$

The concentration of intracellular Ca^{2+} is governed by the calcium balance equation

Equation 3:

$$\frac{d[Ca]}{dt} = \varepsilon(-\mu\, I_{Ca} - k_{Ca}[Ca]).$$

n is a gating variable for the potassium current obeying

Equation 4:

$$\frac{dn}{dt} = \frac{\phi(n_\infty(v) - n)}{\tau_n(v)},$$

$$n_\infty(v) = 0.5\left(1 + \tanh\left(\frac{v - v_3}{v_4}\right)\right),$$

$$\tau_n(v) = 1/\cosh\left(\frac{v - v_3}{2v_4}\right).$$

Synaptic connections between cells are modeled by an equation for the fraction of activated channels

Equation 5:

$$\frac{ds}{dt} = \alpha s_\infty(v)(1 - s) - \beta s,$$

where $s_\infty(v) = 1/\left(1 + \exp\left(-\frac{v+\theta_s}{\sigma_s}\right)\right)$. The term I_{syn} in Equation 1 represents the synaptic current between cells where $I_{syn} = g_{syn}(v - v_{syn})\sum_j s_j$, where the summation is over s

variables from all neurons projecting to a given neuron. Synaptic current for M-cells is $I_{syn,i} = g_{M\to M}(s_j)(v_i - v_{M\to M})$ where $i \neq j$ and $i, j \in \{1,2\}$. Synaptic current for Fast MNs is $I_{syn} = g_{M\to FMN}(s_{M,i})(v - v_{M\to FMN})$ where $s_{M,i}$ is for the corresponding M-cell. Note that right Fast MN receives synaptic input from M-cell 1 while left Fast MN receives synaptic input from M-cell 2. Synaptic current for Slow MNs is $I_{syn} = I_{CPG\to SMN} + I_{IN\to SMN} = g_{CPG\to SMN}(s_{CPG,i})(v - v_{CPG\to SMN}) + g_{IN\to SMN}(s_{IN})(v - v_{IN\to SMN})$ where $s_{CPG,i}$ is for the corresponding CPG and s_{IN} is for i-IN. Note that left Slow MN receives synaptic input from CPG 1 while right Slow MN receives synaptic input from CPG 2. All Slow MNs also get an inhibitory input from i-IN. Synaptic current for i-IN is $I_{syn} = g_{M\to IN}(s_{M,1} + s_{M,2})(v - v_{M\to IN})$ where $s_{M,i}$ is for M-cell i. Synaptic current for CPGs is $I_{syn,i} = g_{CPG\to CPG}(s_{CPG,j})(v_i - v_{CPG\to CPG})$ where $i \neq j$ and $i, j \in \{1,2\}$.

Applied current $I_{app}(t)$ for CPGs and Slow MNs are fixed constants while they are time and activity dependent functions for M-cells, Fast MNs, and i-IN. The applied current $I_{app}(t)$ in M-cell for $i = 1,2$ is modeled as:

Equation 6:

$$I_{app}(t) = I_0 + I_i(\tau) + w_M \times Net(t),$$

where I_0 is a fixed constant, $I_i(\tau)$ is the stimulus at time τ, w_M is a fixed constant for the weight, and $Net(t)$ is the activity-dependent spike adaption in the form of

Equation 7:

$$\frac{dNet'}{dt} = \frac{\left[\frac{ag_{max}}{[Ca]_i} - Net\right]}{\rho}.$$

Here, ag_{max}, ρ are fixed constants and $[Ca]_i$ is the $[Ca]$ for M-cell i.

The applied current in Fast MNs is modeled as:

Equation 8:

$$I_{app}(t) = I_0 + w_{FMN} \times Net(t),$$

where I_0 and w_{FMN} are fixed constants, and $Net(t)$ is as in the above equation, where $[Ca]$ is for each corresponding Fast MN. Note that $Net(t)$ in Fast MNs is not essential as long as the Fast MNs are activated by the M-cells.

Similarly, the applied current in i-IN is modeled as:

Equation 9:

$$I_{app}(t) = I_0 + w_{i-IN} \times Net(t),$$

where I_0 and w_{i-IN} are fixed constants, and $Net(t)$ is as in the above equation, where $[Ca]$ is for i-IN.

For all neurons, the basic set of parameter values are given by the following unless specified in the neuron. We let $g_{Ca} = 4$, $g_{KCa} = 0.25$, $g_K = 8$, $g_L = 2$, $\varepsilon = 0.005$, $v_{Ca} = 120$, $v_K = -84$, $v_L = -60$, $k_1 = 10$, $\theta_s = 0$, $v_1 = -1.2$, $v_2 = 18$, $v_3 = 12$, $v_4 = 17.4$, $k_{Ca} = 1$, $\mu = 0.2$, $c_M = 20$, $\phi = 0.23$. For M-cells, we let $\alpha = 10$, $\beta = 0.08$, $g_{M\to M} = 0.5$, $v_{M\to M} = -50$, $v_4 = 17$, $\delta_s = 4$, $I_o = 40.5$, $w_M = 1$, $I_1(\tau) = 3$, $I_2(\tau) = 0$, $\rho_M = 10000$. For Fast MNs, we let $g_{M\to FMN} = 0.4$, $v_{M\to FMN} = 30$, $I_o = 38$, $w_{FMN} = 0.5$, $\phi = 0.225$, $\rho_{FMN} = 10000$. For Slow MNs, we let $g_{CPG\to SMN} = 0.37$, $v_{CPG\to SMN} = 30$, $g_{IN\to SMN} = 0.7$, $v_{IN\to SMN} = -50$, $I_o = 40.4$. For i-IN, we let $\alpha = 10$, $\beta = 0.0014$, $\phi = 0.225$, $g_{M\to IN} = 0.2$, $v_{M\to IN} = 30$, $I_o = 40.4$, $\delta_s = 1$, $w_{i-IN} = 1$, $\rho_{i-IN} = 4000$. For CPGs, we let $g_{CPG\to CPG} = 0.5$, $v_{CPG\to CPG} = -50$, $I_o = 45$, $\delta_s = 0.2$, $\alpha = 10$, $\beta = 0.2$.

Simulations were performed on a personal computer using the software XPP [12]. The numerical method used was an adaptive-step fourth order Runge-Kutta method with a step size 0.1 ms.

RNA extraction – RNA extractions were performed using a modified phenol-chloroform protocol using Trizol reagent. 400 uL Trizol was added to frozen brain and brain region samples. Samples were homogenized by gentle sonication on ice. 400 uL additional Trizol was added, and then samples were incubated at room temperature for five minutes. 160 uL of chloroform was added, and the samples were mixed by inverting. Samples were incubated at 4 °C for 20 minutes with intermittent mixing, followed by centrifugation at 14,000 rpm, 15 minutes, at 4 °C to separate aqueous and organic phases. The aqueous phase was transferred to a new, sterile tube, and 500 uL of ice-cold ethanol was added. The sample was loaded onto an RNeasy spin column (Qiagen) and spun through at 8000 x g for 30 seconds. Samples were washed with 700 uL buffer RW1, followed by two washes of 500 uL Buffer RPE. RNA was eluted with two, 20 uL volumes of RNase-free water into an RNase-free microfuge tube. RNA extracts were quantified by Nanodrop 2000 (Thermo), and then stored at -80 °C until ready to use

RT synthesis of cDNA stocks – Qiagen's QuantiText Reverse Transcription Kit was used for cDNA synthesis of RNA extracts. Total RNA amounts in the reverse transcription reaction were as follows: 1000 ng for whole brain extracts, 350 ng for telencephalon extracts, 600 ng for hindbrain extracts, 1000 ng for optic tectum extracts, and 450 ng for hypothalamus extracts. RNA was brought to a volume of 12 uL with RNase-free water, and 2 uL Qiagen gDNA wipeout buffer was added. Samples were incubated at 42 °C for two minutes to eliminate any DNA contamination. The following were added to the RT reactions following gDNA wipeout: 1 uL

Quantiscript Reverse Transcriptase enzyme, 4 uL 5x Quantiscript RT Buffer, and 1 uL of oligo-dT and random primer mix from Qiagen. Samples were incubated at 42°C for 30 mins for cDNA synthesis, then three minutes at 95°C for enzyme deactivation. Samples were brought up to a final RNA concentration of 10 ng/uL with RNase-free water and stored at -20°C until ready for qPCR.

qPCR primer design and validation – Primers were designed using NCBI Primer-BLAST software, and are summarized below in Table 1. All primers were designed to span an exon-exon junction, minimize secondary products, produce an amplicon of 75-150 bp, and have an annealing temperature of 60-67 °C. Primers were validated to confirm amplicon size, and to determine ideal primer concentration for qPCR reactions. 20 uL PCR reactions were run using GoTaq Flexi DNA Polymerase Reagents from Promega, and were prepared as follows: 4 uL goTaq Buffer, 2 uL 15 mM $MgCl_2$, 0.4 uL 10 mM dNTPs, varying primer concentrations, 0.1 uL 5 U/uL GoTaq Polymerase, 10 ng of cDNA stock, and sterile water to volume. Primer pairs were assessed at concentrations of 500, 750, and 900 nM final concentrations for amplicon amounts, and the presence of primer-dimer secondary product. PCR reactions were run with the following parameters: 95°C/10min initial denaturation/enzyme activation, 40 cycles of 95 °C/15 second denaturation followed by 60 °C/1 minute annealing/amplification, and then a hold at 15 °C until samples were collected. Samples were run on a 2 % agarose gels, 70 V, for 25 minutes with an Amresco PCR DNA ladder for standardization. Gels contained 0.5x GelRed for visualization under UV light, and pictures were taken with Alpha Innotech's FluorChem 8900 gel imaging system. Working primer concentrations were determined to be: 500 nM for all primer pairs.

Table 1: Primers used for qPCR analysis

Gene	Sequence	Tm (°C)	Amplicon size (bp)	Primer efficiency
actb2	Fw: CCAAACCCAAGTTCAGCCATGG	62.25	118	99.1%
	Rv: TGGATGGGAAGACAGCACGG	62.18		
th	Fw: TTCAGCCATACCAAGACCAG	61.6	147	109.4%
	Rv: CTTCTATGCTGTCCGTGTACG	61.2		
ddc	Fw: ACCCTGATGTGGAACCGGGA	63.05	137	131.7%
	Rv: GTATGGGCTGTGCCAGTGGG	63.18		
slc18a2 (vmat)	Fw: CGGAGGCTGATTCTGTTGATCG	61.37	120	106.4%
	Rv: CATCTGAGCAGCCTCGTCGT	62.28		
slc6a3 (dat)	Fw: AAACACAACGTGGCCCTGGA	62.56	108	90.9%
	Rv: GACTGCCCACACCGAAGAGC	63.39		
drd1b	Fw: TGACAAGGTCTGTGGGAGTACA	63.4	147	104.2%
	Rv: ACGTGAATCGGAGCAACTGG	66.3		
drd2a	Fw: CCTCCATTGTGTCCTTCTACG	62.3	123	93.7%
	Rv: TGTCTGTAACTGGGCATGTG	61.2		
drd2b	Fw: GCTTTCATTCGCCATTTCCTG	66.5	142	93.6%
	Rv: GGTGATAATGAAGGGCACGTAG	63.3		
drd3	Fw: TCTTTGTGACCCTGGATGTG	62.5	140	92.1%
	Rv: CATGACTGAAACCCTTTTGCG	65.4		

qPCR primer efficiency determination – Standard curves for primer efficiencies were prepared using an initial cDNA amount of 30 ng total cDNA, then 1/10 dilutions for amounts of 3 ng, 0.3 ng, and 0.03 ng for a total of 4 difference cDNA amounts. 20 uL reactions of each cDNA amount and each primer pair were run in triplicate on a 96-well PCR plate from Applied Biosystems. Primer pairs were used in predetermined optimal concentrations, and 10 uL 2x Applied Biosystems Fast SYBR green reaction mix was added for a total volume of 20 uL. Real-time PCR reactions were run on an Applied Biosystems Quantistudio 12k Flex Real-Time PCR System for Ct determination. Primer efficiency standard curves were prepared using the Quantistudio 12k Flex Real-Time PCR System software, and are reported above in Table 1.

qPCR reaction protocol – qPCR reactions were run using Applied Biosystems Fast SYBR Green Master mix, using Applied Biosystems Quantiostudio 12k Flex Real-Time PCR System. 96 well plates were used with duplicate technical replicates, and 20 uL reactions were prepared as follows: 10 uL 2x Fast SYBR Green Master Mix, 1 uL of 10 ng/uL cDNA stock, 2 uL 5mM primer pair stock (3 uL 5mM stock for primers using 750 nM final concentrations), and 7 uL RNase-free water (6 uL for primers using 750 nM final concentrations). Reactions protocol was as follows: 95 °C/20 seconds for initial enzyme activation and DNA denaturation, 40 cycles of 95 °C/1 second denaturation followed by 60 °C/20 second annealing/amplification. SYBR green detection occurred during each cycle's amplification stage. Passive reference dye ROX was used for volume standardization. All samples were compared to internal housekeeping gene actb2 for normalization, and isolate fish served as a biological control. Three biological replicates of each social group (Dominant, Subordinate, and Isolate) were analyzed on each 96-well plate. Multiple 96-well plates were run so that each gene had n=10.

qPCR data analysis – qPCR data was analyzed using the comparative ΔΔCt method. All calculations and graphical for qPCR data were performed using a custom computer program developed by the Issa lab. Ct values were determined for each gene of each biological replicate, and experimental genes were compared to internal housekeeping gene actb2 for determination of ΔCt values. ΔΔCt values were determined by normalization of Dominant and Subordinate social groups to Isolate controls, and Fold-change was determined from ΔΔCt values using the appropriate primer efficiencies. Fold-change values were transformed to a log base 2 scale for graphing and statistical analysis. Individual gene's fold changes were analyzed for significance by two-sided one sample t-test from a theoretical mean of 0, while fold changes between social groups (Dominant and Subordinate) were analyzed using a two-sided Wilcoxon signed rank test, $\alpha = 0.05$.

RESULTS

Zebrafish form stable social hierarchies

Paired zebrafish quickly form stable dominance relationships. We observed the social agonistic interactions of paired adult male zebrafish daily and counted aggressive (attacks) and submissive (retreats) behaviors performed by each fish for the pairing period. Dominance relationships were established by the third day of interactions and remained stable for the remainder of two weeks of observation. During this period the dominant animal of each pair performed most of the aggressive chasing and biting behavior (Figure 4A, top), while the subordinate mainly retreated from interactions (Figure 4A, bottom).

Social status-dependent regulation of swimming behavior

Paired zebrafish showed significantly different swimming tendencies based on the animal's social rank. Dominant animals swam freely around their tank enclosure, while subordinate fish preferred the shelter of the bottom corner of the tank (Figure 4B). The density plot in Figure 4B illustrates the spatial probability distribution of all animals observed over 1 min of filming sampled at three frames/second on day 12 of the pairing period. To quantify this observation, we measured the average distances swum for each day of pairing for a 1-minute interval for 14 consecutive days (Figure 4C). We performed a two-way ANOVA to test differences in swimming activity by social rank (factors: group and day). There were significant main effects of group [$F(2, 535)=2.11e+2$, $p<1.0e-16$, Figure 4C] and day [$F(14, 535)=3.12$, $p=1.02e-4$, Figure 4C]. There was also an effect of interaction between group and day [$F(28, 535)=2.93$, $p=1.21e-6$, Figure 4C]. In particular, we observed that the normalized swim distance of Dominants was significantly longer than those of group-housed and Subordinates

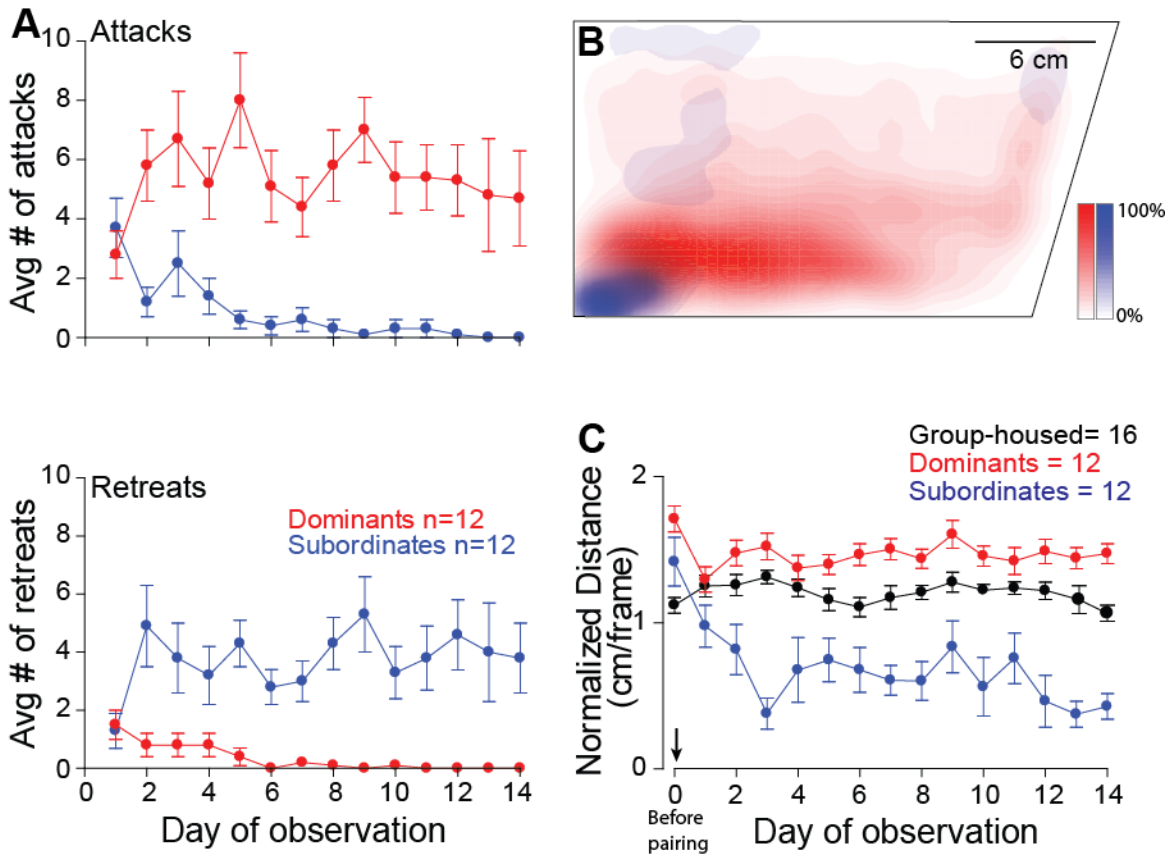

Figure 4 – Zebrafish form stable social hierarchies with divergent behavior

Adult male zebrafish form stable social relationships and behavior patterns diverge significantly as social relationships solidify. A) Social interactions are characterized by aggressive behaviors (attacks, top graph) performed predominantly by dominants and submissive behaviors (retreats, bottom graph) displayed mainly by subordinates. B) Social status affects swimming activity. Kernel heat-map estimation plot of swimming activity over a 1 minute period of filming for Dominants (red) and subordinates (blue) on day 12 post pairing (n=12 Dominants and 12 subordinates). C) Quantification of filmed swimming activity [distance traveled (cm)/frame] for all animals tested during a 1 minute period, each day for a 14 day pairing period. Video frames during which the animals were interacting were excluded from analysis. Total tracked distance was normalized by the number of remaining video frames. Day 0 marks observations of animals before they were paired (Before pairing: arrow).

[Tukey HSD, p≤9.56e-10, Figure 4C] and the normalized swim distance of group-housed animals was also significantly longer than that of Subordinates [Tukey HSD, p=9.56e-10, Figure 4C]. That is, Subordinates significantly decreased their swimming activity as dominance was formed. This decline of swimming persisted for the remainder of pairing. Conversely, Dominant animals increased their swimming activity in comparison to group-housed animals (Figure 4C, B; n=12 for Dominants and Subordinates each, and n=16 for group-housed animals).

Secondly, we measured the animals' swim burst activity. Animals were tested individually by placing them in the testing chamber described above and recorded spontaneous swimming bursts field potentials for 1 minute after a 30 minutes period of acclimatization on day 12 of pairing (Figure 5A). We found similar results with swim bursts as with swimming activity in the housing tanks: dominant animals swam more than group-housed and subordinate animals (Figure 5B, C). We performed a two-way ANOVA (factors: group and time bin) to compare the average number of bursting swim activities. There was significant main effect of group [F(2, 480)=5.45e+1, p<1.0e-16, Figure 5C] while there was no effect of time bin [F(11, 480)=9.70e-1, p>0.05, Figure 5C]. We observed that the average number of bursting swim of Dominants was significantly higher than those of group-housed and Subordinates [Tukey HSD, p≤1.36e-9, Figure 5C] and the average number of bursting swim of group-housed was significantly higher than that of Subordinates [Tukey HSD, p=1.19e-4, Figure 5C]. We also compared the total number of swim bursts with one-way ANOVA (factor: group). We found a significant main effect of group [F(2, 40)=1.49e+1, p=1.48e-5, Figure 5C]. Dominants showed a significantly higher number of bursting swim compared to group-housed and subordinate animals [Tukey HSD, p≤4.87e-3, Figure 5C]. While Dominants substantially increased their bursting swim activities compared to both group-housed and subordinate fish, Subordinates

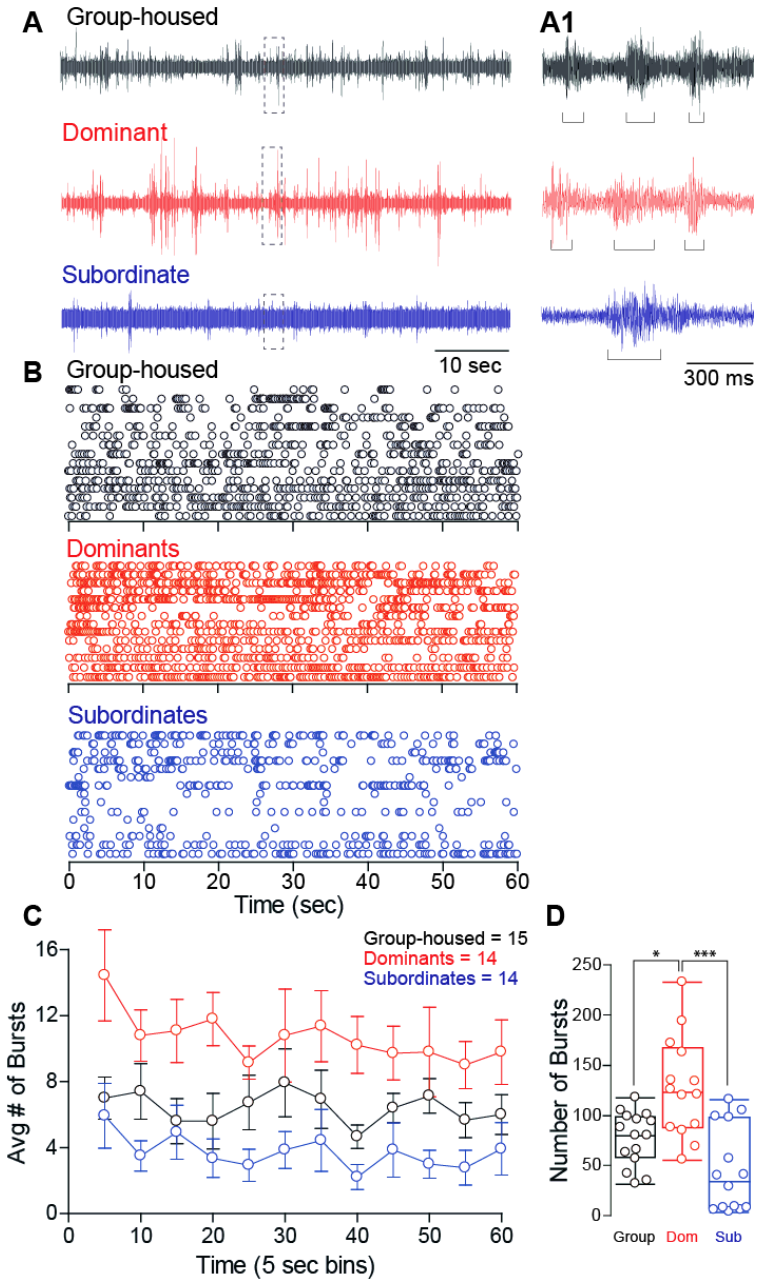

Figure 5 - Social status affects swimming burst frequency

1 minute individual trace recordings of field potentials from group-housed, dominant and subordinate animals. Swim bursts are easily identifiable and individually sorted (A1, brackets) (dashed boxes denote areas that are enlarged in part A1). B) Raster plots of each social animal group tested. Each row represents the burst swim responses of one animal, and each circle represents one swim burst (see methods for burst analysis and quantification). C) Averaged binned data of swim burst activity of data illustrated in part A and B. (burst activity was binned over 5 seconds). D) Box plot summary illustrating differences in the number of bursts produced over 1 minute of recording. Each dot represents sum of spontaneous swim bursts for each animal during 60 sec of recording. Horizontal line within each boxplot denotes data median, box represents 90% of data. Error bars represent max/min values.

significantly decreased their bursting swims from those of group-housed and Dominants (Figure 5C, D). These results suggest that social interactions have impacted the swim circuit of both dominant and subordinate animals but in opposing ways. Social dominance caused an increase in swimming while social submission led to a decrease in the activity of the swim circuit.

Social status affects C-start escape response

To determine whether social experience affects the activation threshold of the M-cell escape, we tested the animals' sensitivity to auditory pulses of randomized decibel intensities. At low decibels, both social phenotypes displayed similarly low response probabilities (Figure 6A). However, as sound intensity increased subordinates were significantly more sensitive and were more likely to respond to auditory pulses compared to Dominants and group-housed animals (Figure 6B). Subordinate animals response probability reached the 50% mark at 82.73 dB compared to Dominants of 86.86 dB and group-housed animals 85.30 dB (One-way ANOVA with Newman-Keuls Multiple Comparison Test, two-tailed, *P=0.0091* at 85 dB and *P=0.0344* at 90 dB). Data was curved fitted with a non-linear regression with Boltzmann Sigmoidal curve fit; Goodness of fit R^2 for group-housed= 0.9868, Dominants= 0.9924, Subordinates= 0.9926; Group-housed n=20; Dominants n=23; Subordinates n=23). At supra-threshold stimuli (95dB and higher) the response probability of animals plateaued to similar levels. Comparison of the sensitivity curves of dominant and subordinate animals to group-housed shows that paired-wise interactions had a significantly bigger impact on the response sensitivity of socially subordinate animals compared to Dominants (Figure 6B). Our results suggest that the activation threshold of the M-cell in Subordinates decreased significantly compared to both dominant and group-housed animals

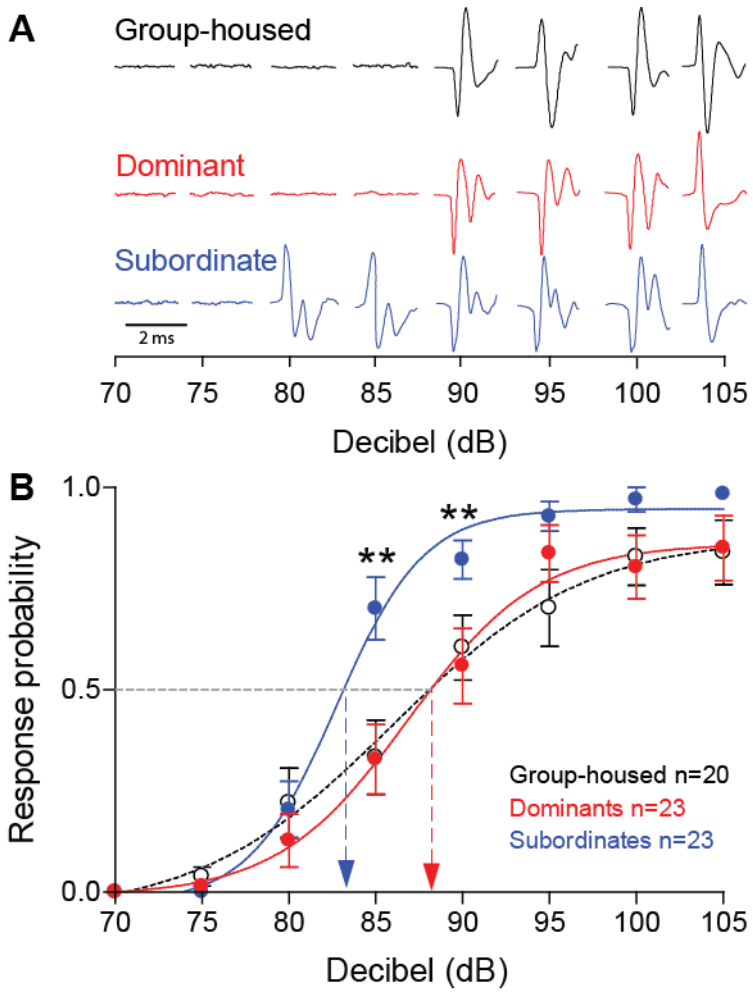

Figure 6 – Social status affects startle escape probability
Startle escape response is significantly more sensitive in subordinate animals compared to dominant and group-housed animals. A) Individual examples of c-start field potential from 3 different animals at increasing decibel intensities. B) Probability of initiating an escape response is significantly higher in Subordinates compared to Dominants and Group-housed at 85-90dB. A response probability of 0.5 is indicated with the dotted line

Model to illustrate behavioral changes

To investigate the mechanisms underlying the status-dependent differences in startle sensitivity and shift in network activation between escape and swim we built a simplified mathematical neural model of both escape and swim circuits (Figure 7A). We found that a simple circuit model composed of conductance-based modified Morris-Lecar neuronal model neurons can account for the observed social status differences in circuits' dynamics. The model incorporates the main neural elements that comprise the M-cell escape circuit, a swimming central pattern generator (CPG) circuit, an inhibitory i-IN, Fast and Slow MNs that are connected to the M-cell escape and CPG swim circuits, respectively (see Materials and Methods for detail). It is well established that the excitability of the escape and swim circuits is subject to descending neuromodulation [76, 78]. However, it is little understood how a change in the M-cell excitability alters circuit activation and promote a switch between escape and swim. Here, we hypothesized that modulation of network properties may account for the observed differences in circuit activation between Dominants and Subordinates. To test our hypothesis we controlled two intrinsic synaptic parameters, the maximal net excitabilities in the M-cell, Fast MN and i-IN, which are modulated by presynaptic neurotransmitters.

We repeatedly applied depolarizing current pulses to the model M-cell (1 sec inter stimulus interval) for 100 ms duration on the left M-cell to explore the behavior of the escape and swimming activities for each animal group (Figure 7B). We changed ag_{max} in $Net(t)$ (Equations 6, 8, 9) and the weight w_{i-IN} for i-IN in $I_{app}(t)$ (Equation 9). Using empirical data to inform our model, we assumed that low values of ag_{max} and w_{i-IN} correspond to the dominant and communal fish while the high values of ag_{max} and w_{i-IN} correspond to the subordinates.

Figure 7 - Neurocomputational model of the escape and swim circuits

A) A schematic illustration of the model neural network that reproduces the responses observed in group-housed, dominant, and subordinate animals. The M-cell (M: green) excites the Fast MNs and inhibitory interneurons (i-IN: blue). Each M-cell mutually inhibits its homolog. The swim CPG (Red) excites the Slow MNs.

B) Activities of model M-cell (top row), fast MN neurons (middle row) and slow MN neurons (bottom row) for the three animal groups to repeated depolarizing current stimulation injected into the left M-cell (repeated 18 times; 1 sec inter stimulus interval) with100 ms duration (B11, B21, B31) dominant animals with $ag_{max} = 4.5$ and $w_{i-IN} = 1$. (B12, B22, B32) group-housed animals with $ag_{max} = 4.7$ and $w_{i-IN} = 1$. (B13, B23, B33) subordinate animals with $ag_{max} = 9.5$ and $w_{i-IN} = 2.25$. Upper panels, the green spikes represent the active (left) M-cell while the red line represents the silent (right) M-cell. "[Net]" in the insert represents the total amount of excitability of the M-cells, i-IN and Fast MNs: low (Dominants), intermediate (Group-housed), and high (Subordinates). In the middle panels (B21-23), the green line represents the active right Fast MN while the red line represents the silent left Fast MN. In the bottom panels (B31-33), the green line represents left Slow MN while the red line represent right Slow MN.

C) A change in the amplitude of the applied current $I_1(\tau)$ and the response rate of M-cell to the 18 stimuli for three animal groups.

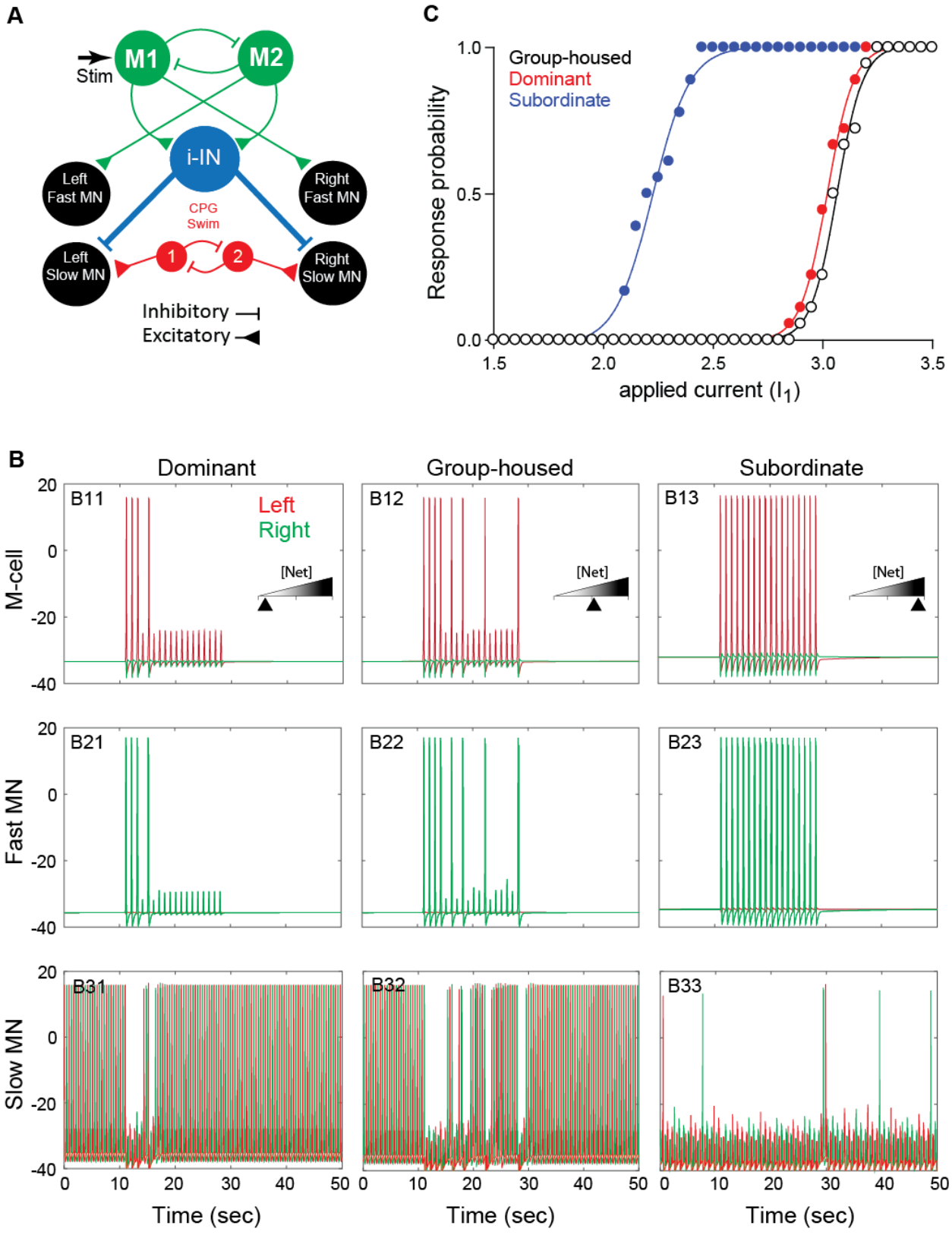
A
M1
M2
Stim
i-IN
Left Fast MN
Right Fast MN
CPG Swim
1
2
Left Slow MN
Right Slow MN
Inhibitory
Excitatory
C
Group-housed
Dominant
Subordinate
Response probability
1.0
0.5
0.0
1.5
2.0
2.5
3.0
3.5
applied current (I_1)
B
Dominant
Group-housed
Subordinate
B11
B12
B13
Left
Right
[Net]
M-cell
B21
B22
B23
Fast MN
B31
B32
B33
Slow MN
20
0
-20
-40
0
10
20
30
40
50
Time (sec)

Switch between escape and swimming activities

Figure 7B shows the activities of neurons (M-cells, Fast MNs, and Slow MNs) for all three animal groups. A depolarizing current pulse that activates the M-cell (Figure 7 B11, B12, B13) leads to the activation of the contralateral Fast MNs (Figure 7 B21, B22, B33; right Fast MN) and initiation of the escape response. Concurrently, activation of the M-cell excites the i-IN, which directly inhibits all Slow MNs. As a result, there is a pause of swimming activity during escape, but swimming resumes once the escape response ends (Figure 7 B31, B32, B33).

Effect of social status on the swimming activity in the model

To determine how social experience may account for the observed changes in swim circuit activation, we tested the activities of Slow MNs before, during and after repeated stimulation of the M-cell. The bottom panels in Figure 7B shows the response of Slow MNs of models that simulated responses of dominants (Figure 7 B31), communals (Figure 7 B32), and subordinates (Figure 7 B33) without any stimulus input (before 10 seconds and after 30 seconds). Then we increased parameter values ag_{max} and w_{i-IN} to determine the effect on swimming behavior. As described earlier, low ag_{max} and w_{i-IN}values simulate conditions that represent communals and dominants while high values represent subordinates. We found that swimming frequency before and after the stimuli did not change for each animal group. We also observed that Slow MNs for communals and dominants were active most of the time except during activation of escape circuit. On the other hand, increasing ag_{max} and w_{i-IN} led to a dramatic decrease in swim circuit activation prior, during and after escape circuit activation for subordinates (Figure 7 B33). This result mimics our empirical results that show an inhibition of swimming activity in subordinate animals (Figure 4 & 5).

Social status-dependent sensitivity of M-cell escape response in the model

To probe possible cellular mechanisms that account for the observed social status-dependent changes in the sensitivity of the M-cell we changed the amplitude of the applied current in M-cell and measured the response probability over the repeated stimuli. As in the previous simulation, the left M-cell receives 18 stimuli. Amplitude of the applied current $I_1(\tau)$ was gradually increased, and response probability of M-cell was recorded. For example, the response probabilities of M-cells in Figure 7 upper panels are 4/18 for Dominants, 8/18 for Group-housed, and 18/18 for Subordinates. We used the same parameters as in the above simulation for each animal group. We found that decreasing ag_{max} and w_{i-IN} increases the activation threshold of the model M-cell as observed in dominant and group-housed animals. But when ag_{max} and w_{i-IN} values were increased the activation threshold of the model M-cell decreased significantly as we observed experimentally in subordinate animals (Figure 7C). Taken together, these results suggest that social status-dependent changes in the M-cell may be mediated, in part, by intrinsic changes in M-cell excitability and are sufficient to enhance the escape response and to switch circuit activation from swim to escape as was observed experimentally (Figure 5C, 6B)

Social status affects whole brain gene expression of DA genes

To determine the effects of social status on DA signaling, patterns of gene expression of enzymes involved in the synthesis, transport, packaging, release and reuptake of DA were measured in addition to the gene expression of DA receptors. We found that dominant and subordinate animals show differential expression of whole brain DAT and D1R-related genes (Figure 8B). Levels of DAT are significantly higher in Dominants compared to Subordinates (Wilcoxen Signed Rank Test, $p < 0.01$), with both social groups showing significantly more

DAT expression than Isolates (one-sample t-test, $p < 0.01$). Levels of D1R are also higher in Dominants versus Subordinates (Wilcoxen Signed Rank Test, $p < 0.05$) with both social groups showing significantly less D1R expression than Isolates (one-sample t-test, $p < 0.01$). In addition to these differentially expressed genes, we found that both dominant and subordinate fish showed increased expression of DDC compared to Isolate controls (one-sample t-test, $p < 0.05$ for Dominants; $p > 0.01$ for Subordinates). Whole brain expression analysis serves to show that there is, indeed, a social-status dependent effect on the expression of DA associated genes.

Regional differences in DA signaling gene expression

Two brain regions of interest were examined due to their anatomical and functional connectivity with the Mauthner escape circuit: The hypothalamus, containing DA neurons thought to project to the vicinity of the Mauthner cell, and the hindbrain, the physical location of the pair of Mauthner command neurons (Figure 8A). Neither region showed significant changes in expression of the DA-related genes compared to Isolates, or due to social status. Since the significant changes in expression of DAT and D1 found in whole brain samples were not found in either the hindbrain or hypothalamus, the changes in expression of these are likely occurring outside of these regions.

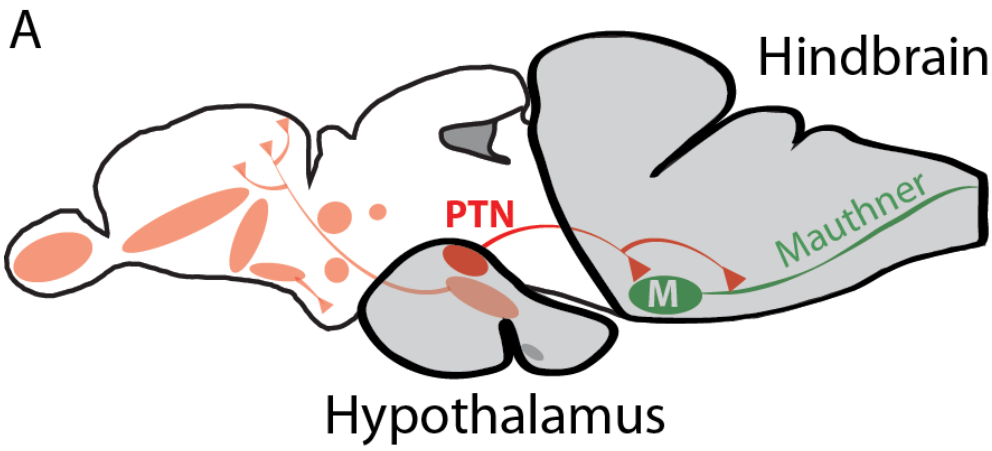

Figure 8 - Relative quantity of Dopamine associated gene expression
[Above]
A) Schematic of zebrafish brain and regions used for gene expression analysis. DA nuclei labelled in red, M-cell in green. PTN= posterior tuberal nucleus (see discussion for details).

[Below]
Expression of DA genes in the B) whole brain (n=10) C) hindbrain (n=6) and D) hypothalamus (n=6) by qPCR using the ΔΔCt method. Beta actin (actb2) used as an internal reference gene, and expression from social isolates used for standardization. Individual animal data shown as points for each gene. Bars represent mean and SEM for data set. Fold changes transformed to a log base 2 scale for statistical analysis and more accurate representation of expression change data. Zero indicates no change in gene expression relative to isolate controls. Expression differences between Dominants and subordinates calculated by Wilcoxen signed rank test. Expression differences between expression and Isolate controls were calculated by one sample t-test. [p-values: * < 0.05, ** < 0.01]

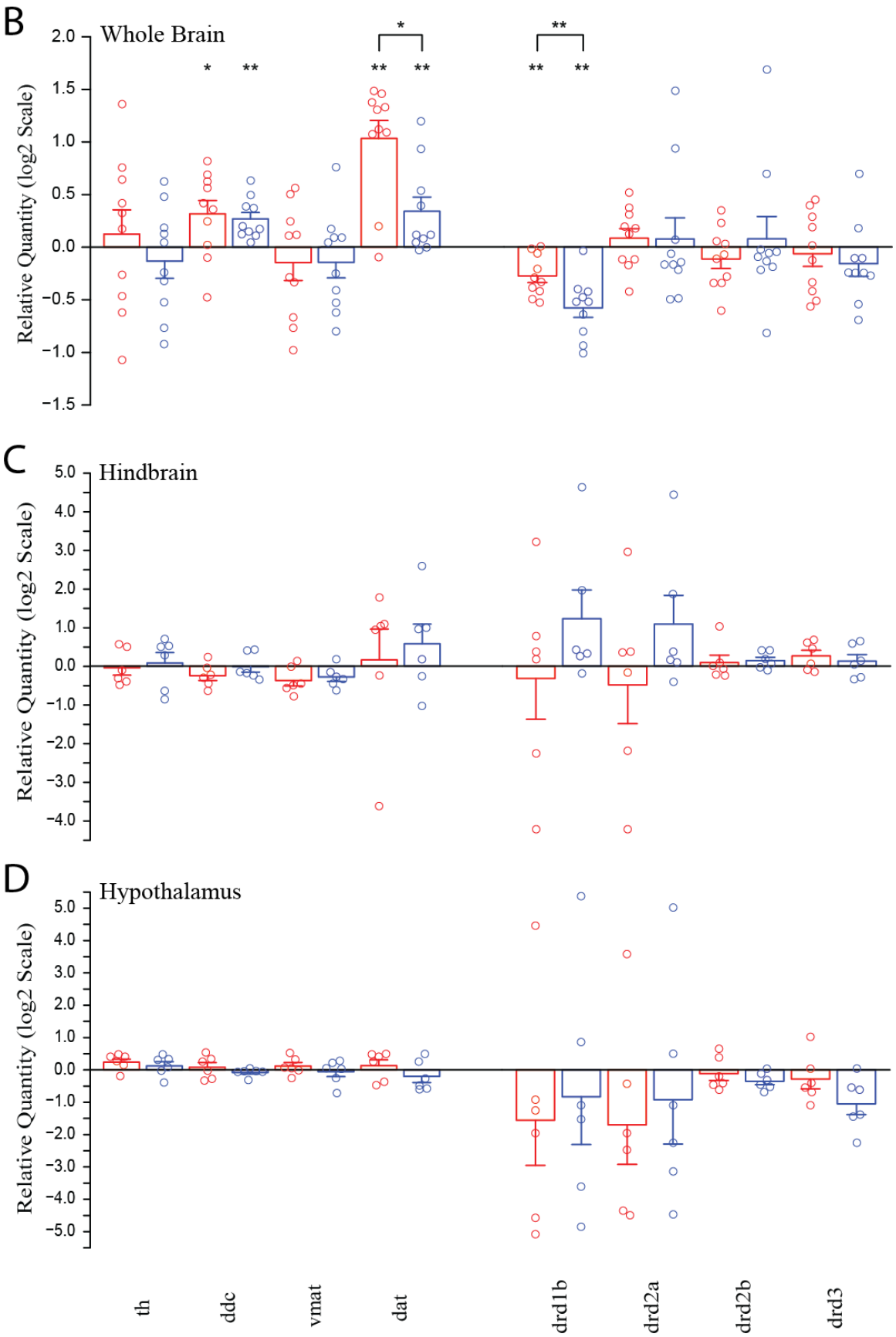
B
Whole Brain
Relative Quantity (log2 Scale)
2.0
1.5
1.0
0.5
0.0
−0.5
−1.0
−1.5
*
**
**
**
*
**
**
**
C
Hindbrain
Relative Quantity (log2 Scale)
5.0
4.0
3.0
2.0
1.0
0.0
−1.0
−2.0
−3.0
−4.0
D
Hypothalamus
Relative Quantity (log2 Scale)
5.0
4.0
3.0
2.0
1.0
0.0
−1.0
−2.0
−3.0
−4.0
−5.0
th
ddc
vmat
dat
drd1b
drd2a
drd2b
drd3

DISCUSSION

Our results show that social experience affects decision-making and the potential for activation of the neural circuits that underlie escape and swimming in male adult zebrafish. A shift in the balance of networks dynamics favors increased probability of activation of the escape circuit over utilization of the swim circuit in subordinate animals; while in dominant animals swim circuit activity is promoted over escape potential (Figure 9). To determine possible cellular mechanisms that account for the observed status-dependent differences, we built a neural circuit model of the escape and swim circuits based on a simplified representation of the properties of the relevant neurons. Although our simplified model circuit does not include all the detailed neural elements that may act *in vivo*, we were able to reproduce several important network activity patterns observed experimentally. A change in intrinsic synaptic (M-cell excitability) and network parameters (strength of the connection of the M-cell to inhibitory elements) was sufficient to obtain the transition between dominants and subordinates activity patterns while keeping the network architecture. It is known that the escape and swimming circuits are prone to behavioral and cellular plasticity mediated by modulatory inputs [49, 58, 64, 66]. Therefore modulation of network properties by neurotransmitters may be responsible for the empirically observed changes in startle sensitivity between Dominants and Subordinates. The M-cell is responsive to 5-HT, DA, GABA, and Glycine [33] and one or a combination of these neurotransmitters could change its cellular properties. This study focused on the implications DA, but investigating 5-HT and inhibitory neuromodulation could be important for determining what is occurring in this system in-vivo.

Social status was sufficient in changing whole brain RNA expression of dopamine D1 receptor (D1R), the dopamine transporter (DAT), and L-Dopa decarboxylase (DDC) in dominant

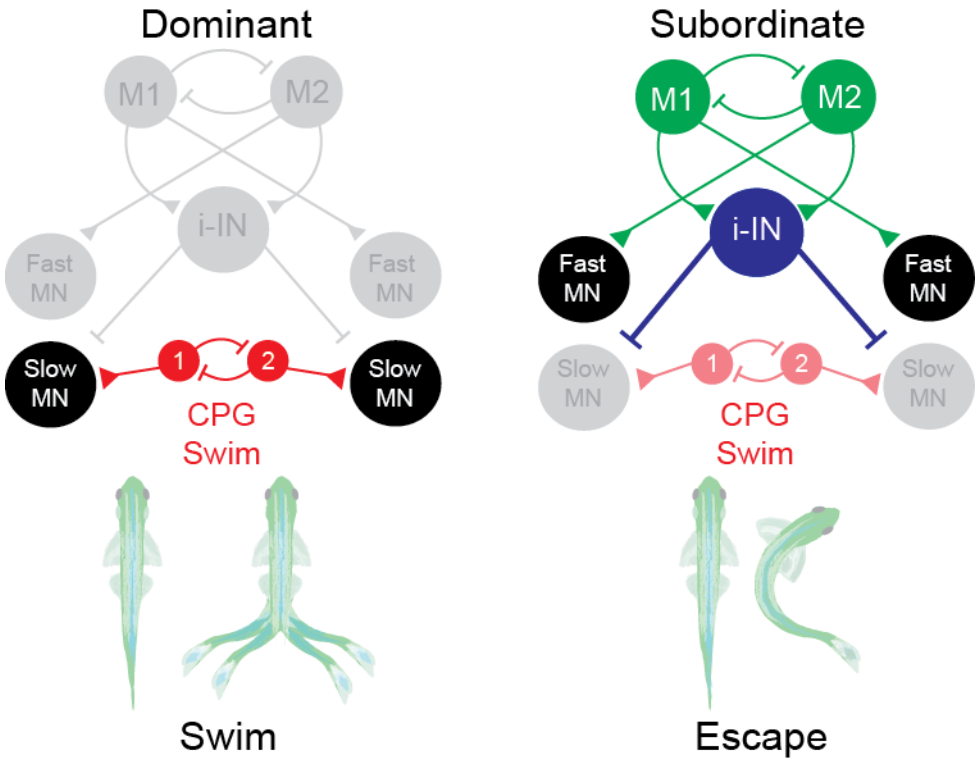

Figure 9 – Proposed schematic illustrating the shift in motor network activation
Our results suggest a shift in activation between escape and swimming in socially Dominant and Subordinate animals is occurring. In Dominant animals, a low or absence of the inhibition from inhibitory interneurons with the continuous excitatory input from swim CPG potentiates swimming activity. However, in Subordinate animals, an increase in excitability of the inhibitory neurons suppresses the Slow MNs and swimming behavior. Simultaneously, an increase in Mauthner sensitivity promotes the excitation of the escape circuit and inhibition of swim circuit. Suppressed pathways are dimmed, while synaptic pathways that are strengthened are colored emphasized.

and subordinate animals compared to controls. While we did observe changes in RNA expression, it is important to note that these changes may not reflect changes in protein levels within these animals. Therefore an examination of proteins expression of these differentially expressed genes would be an important next step in this process. The supply of DA in the nervous system depends on de-novo synthesis of DA by TH and DDC, recycling of synaptic DA by DAT, and the degradation of DA by COMT and MAO. Changing any of these factors could alter available DA levels which would alter DA's effect on its target neurons. Increased expression of DDC could result in socially dominant or subordinate fish having more DA available in synaptic vesicles than Isolated controls. However, it has been demonstrated that Dominant and Subordinate animals do not show significant differences in fore- and hindbrain DA levels and the DA metabolite 3,4-dihydroxyphenylacetic acid (DOPAC) following 5 days of social interactions [9]. Therefore the synthesis and degradation of DA are unaltered due to social status. However, DDC is also a critical step in the synthesis of 5-HT, indicating that serotonin may also be socially regulated in this system.

If the supply and degradation of DA are not being altered due to social status, the increased level of DAT expression found in dominant fish would be the major determinant behind synaptic DA supply. Higher expression of DAT in dominant animals would result in an increased rate of DA recycling, and therefore DA would have a shorter presence within the synapse. The attenuation of DA in the synapse may be important for the proper formation of stable social hierarchies and reducing aggressive acts after a dominance relationship has been established. Mice lacking DAT [DAT (-/-)], and therefore unable to recycle synaptic DA properly, show an increase in spontaneous hyper-locomotion [26] and a preference for aggression over mild social interactions [61]. These DAT (-/-) mice did not reduce their

aggressive behavior even after repeated exposure to familiar animals indicating that they were unable to adapt to a social context. In our study, aggressive attacks decreased over time once dominance is stabilized (Figure 4A) implicating that the attenuation of DA in the nervous system may be important for the reduction of aggressive acts as social hierarchies solidify.

Both supply and interpretation of the DA signal are important in determining how the behavioral output will be modulated. Therefore changes in the types and amounts of DA receptors expressed in the brain play an important role in the ultimate effect of DA signaling in the brain. We have found that 2 week of social interactions result in dominant and subordinate fish having decreased D1 expression compared to isolates, with the decrease in subordinate being greater. Previous studies suggest that visual stimulation of larval zebrafish can modulate the sensitivity of the Mauthner circuit, mediated through D1-like receptor signaling in the caudal hypothalamus, supporting the notion that D1 could play a major role in shaping Mauthner escape sensitivity [45, 67]. Application of the D1 antagonist SCH 23390 in zebrafish resulted in an increased escape sensitivity and a decrease in swimming of Dominants or causing them to behave more like a Subordinate animal [7]. Since D1 mediates excitatory actions in post-synaptic cells, it could be assumed that antagonizing D1 should lead to a decrease in M-cell excitability [7]. However, these conflicting results suggest the possibility that D1 signaling to the M-cell may be working through an intermediate inhibitory interneuron rather than acting directly on the M-cell. D1 has been investigated in the context of social aggression in other species as well as zebrafish. In mammals, pharmacological blockage of the D1 receptor during social interactions has been shown to cause a facilitation of social dominance in mice and an alteration of social affiliative relationships in non-human primates [73]. These results indicate that D1 is an important substrate for social interactions and the development of socially adaptive behaviors.

Taken together, the changes in DDC, D1, and DAT expression in Dominant and Subordinate zebrafish suggest that mechanisms behind DA modulation of motor activity extends beyond the types of receptors expressed. Therefore studies that examine only the function of DA receptors as they relate to a behavioral function may be incomplete. An examination of the synergistic interactions of the supply and interpretation of DA are important considerations to keep any behavioral modulation in context.

Another important determinant into DA function within the brain is the location of the putative changes in DA supply and/or its interpretation. In order to address regional changes in DA function we examined the expression of the same DA-related genes in the hypothalamus (putative origin of the DA supply for the escape and swim circuitry) and the hindbrain (physical location of the M-cell and MLR nuclei). We observed no significant changes in expression of any DA-related genes within these two regions (Figure 8C, D). Given that the significantly different expression observed for DDC, DAT, and D1 in whole brain tissue were not observed in these regions, it is likely that the expression changes are occurring elsewhere. Two brain regions not tested in this study were the optic tectum and the forebrain (telencephalon). The forebrain contains both DA nuclei and DA responsive cells which send projections to various cell groups in the nervous system, including the VTA nuclei in the hypothalamus. The Optic Tectum DA responsive cells are responsible for the processing and interpretation of visual information in zebrafish, making it a potentially vital relay station for the integration of visual social cues in the formation of social hierarchies (discussed in Chapter 3). Both of these regions are viable options for further investigation into social status-dependent neuromodulation in zebrafish.

CHAPTER III

IMPORTANCE OF VISUAL CUES FOR BEHAVIORAL SELECTION

INTRODUCTION

An import aspect of a social dominance is the ability of individuals to send and receive information about social status [21]. This outward display of social rank is crucial for the stability of social hierarchies, and to reduce conflict for resources and dominance within a social group [22]. The types of social rank cues that individuals send to their conspecifics are various, but of particular interest are visual cues. Using visual cues to display social dominance or to attract mates is a common theme from non-human primates to fish [62]. In Teleost fish, the role of visual cues in the formation of social hierarchies has been studied in various fishes like rainbow trout (*Oncorhynchus mykiss*) [21, 25], cichlid fish (*Astatotilapia burtoni*) [31], and artic charr (*Salvelinus alpinus*) [20]. Body coloration in cichlid fish is socially regulated such that dominant animals are conspicuously brighter in coloration compared to subordinates [31]. Consequently, higher selective pressure in the form of increased predation of dominants is likely to occur. As with zebrafish, the M-cell in cichlid displays behavioral and cellular plasticity [42]. Interestingly, unlike zebrafish, the response of the M-cell in dominant cichlid is significantly enhanced compared to subordinates [46] suggesting species-dependent adaption to different ecological constraints.

Visual Cues in Zebrafish

Although zebrafish have not been documented to undergo an obvious change in body coloration during social interactions, stripe patterns are important in the normal schooling behavior of zebrafish communities [46]. In addition, zebrafish have been shown to alter their melanophore (dark pigment) production based on their environment [37]. Later studies

confirmed that melanophore changes were not only a physiological response, but also could be improved by cyclical training, and therefore a learned response [18]. Visual information also acts as a neuromodulator in zebrafish; visual stimuli have been shown to enhance the excitability of the M-cell and reticulospinal neurons via descending dopaminergic input. Larval zebrafish respond to threatening visual stimulus by inactivating hypothalamic dopaminergic neurons and their positively regulated hindbrain interneurons, resulting in dis-inhibition of C-start escape generation [76]. This revealed that neuromodulation can be tuned by visual cues in order to help animals generate appropriate behavioral responses. It has also been demonstrated that light induced modulation of the escape response by hypothalamic DA neurons occurs through a D1 mediated pathway [45]. In addition, neurons in the medial longitudinal fasciculus (nMLF) which are crucial for locomotor output in larval zebrafish were strongly activated during light-evoked swimming demonstrating that they are potentially modulated by visual input [64]. In order to assess the importance of socially displayed visual information in the formation of social hierarchies in zebrafish, we took advantage of a strain of zebrafish that lack pigmentation: the Tupfel long fin nacre (TLN) line.

TLN zebrafish as a model for the importance of visual cues

TLN fish are produced by causing two homozygous mutations in an Tubingen background: First a homozygous recessive mutation in the connexin 41.8 (cx41.8) gene causes spotting of pigment cells in adult zebrafish resulting in the Tupfel long fin (TL) phenotype; second, homozygous mutations were introduced into the microphthalmia-associated transcription factor a (mitfa) gene which is essential in melanophore development [36], resulting in the TLN line. These TLN fish are completely lacking in dark pigmentation on the side of the fish, and

therefore are ostensibly unable to convey visual cues to conspecifics. Given their lack of visual displays, we hypothesize that paired TLN fish may be unable to form stable social hierarchies. In addition, given that visual priming plays an important role in the modulation of the M-cell and swimming circuitry, the lack of visual cues by TLN fish may prevent the social-status dependent changes in behavior observed in AB fish.

Here we paired adult male TLN fish, and measured their escape response sensitivity and swimming behaviors as performed on AB fish in Chapter II. We found that TLN fish do appear to form stable social hierarchies, albeit with a higher prevalence of pairs that switch their social status during the pairing period. Secondly, we found that TLN fish drastically alter their swimming behavior compared to AB fish, showing no social status-dependent place preference or differences in overall swimming activity. Lastly, we will show that TLN fish do not alter the sensitivity of their C-start escape response based on social rank.

EXPERIMENTAL METHODS

Methods used for TLN are identical to those listed in Chapter II

Adult TLN fish were maintained at 28°C, pH 7.3, and fed in excess three times daily. Group-housed TLN males were placed into isolation for one week and then paired for a two week period as before. TLN pairs were filmed to measure swimming activity and place preference as described on pages 11-12. In addition, swim burst activity and escape response were measured as described on page 13.

RESULTS

Lack of visual cues decrease stability of social hierarchies

Paired TLN form less stable dominance relationships than AB fish. We observed the interactions of paired adult male TLN zebrafish and counted aggressive and submissive attacks for each day of the pairing period. During this period the dominant animal of each pair performed most of the aggressive chasing and biting behavior (Figure 10A, top), while the subordinate mainly retreated from interactions (Figure 10A, bottom). On average, as was observed with the wild-type zebrafish dominance relationships were established by the third day of interactions. However, approximately a third of TLN pairs observed (n= 5/16) switched their social status at least once during the pairing period. This result suggests that visual information is important in regulating social interactions and stability of social relationships.

Lack of visual cues eliminate social status-dependent effect on swimming behavior

Paired TLN zebrafish did not show significantly different swimming tendencies based on the animal's social rank. Both Dominant and Subordinate animals swam freely around their tank enclosure (Figure 10B). The density plot in Figure 10B illustrates the spatial probability

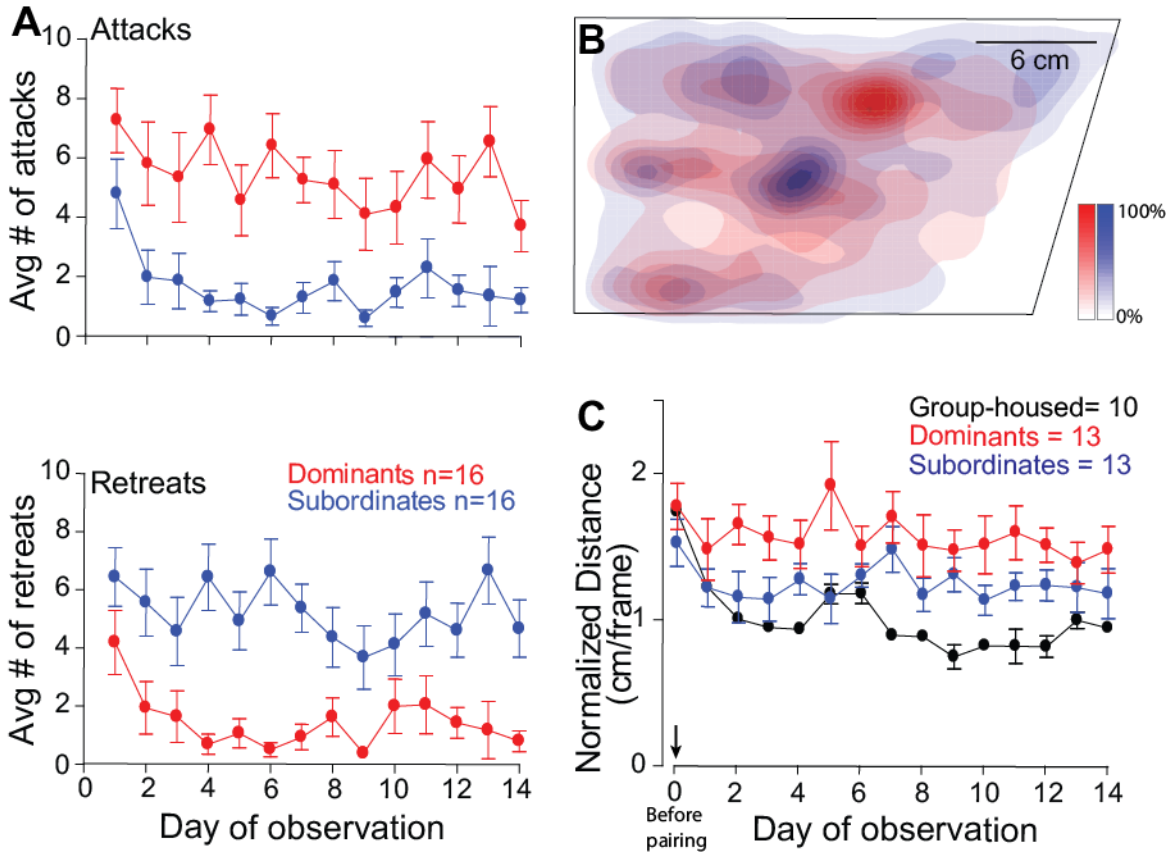

Figure 10 – Lack of visual cues eliminate social rank differences in swimming

Adult male TLN zebrafish can form stable social relationships. A) Social interactions are characterized by aggressive behaviors (attacks, top graph) performed predominantly by dominants and submissive behaviors (retreats, bottom graph) displayed mainly by subordinates. B) Social status does not affect swimming activity in TLNs. Kernel heat-map estimation plot of swimming activity over a 1 minute period of filming for Dominants (red) and subordinates (blue) on day 12 post pairing (n=12 Dominants and 12 subordinates). C) Quantification of filmed swimming activity [distance traveled (cm)/frame] for all animals tested during a 1 minute period, each day for a 14 day pairing period. Video frames during which the animals were interacting were excluded from analysis. Total tracked distance was normalized by the number of remaining video frames. Day 0 marks observations of animals before they were paired (Before pairing: arrow).

distribution of all animals observed over 1 min of filming sampled at three frames/sec. To quantify this observation, we measured the average distances swum by TLN fish for each day of pairing for a 1-minutes interval for 14 consecutive days (Figure 10C). We performed a two-way ANOVA to test differences in swimming activity by social rank in TLN fish (factors: group and days). There were significant main effects of group [$F(2, 397)=42.38$, $p<0.0001$, Figure 10C] and days [$F(14, 397)=1.840$, $p=0.0314$, Figure 10C], but no effect of interaction between group and days [$F(28, 397)=0.7060$, $p = 0.8674$, Figure 10C].

Visual Cues prime social status effect on C-start escape response

To determine whether social experience affects the activation threshold of the M-cell escape in TLN fish, we tested the animals' sensitivity to auditory pulses of randomized decibel intensities. Dominant and subordinate animals showed similar response probabilities regardless of sound intensity (Figure 11A). Animals' response probabilities were similar regardless of social status: Subordinates reached the 50% mark at 81.18 dB, Dominants at 79.08 dB and group-housed animals at 80.7 dB. Data was curve fitted with a non-linear regression with Boltzmann Sigmoidal curve fit; Goodness of fit R^2 for group housed = [0.8091], Dominants = [0.7709], Subordinates = [0.6927]; group-housed n = 13; Dominant n = 12, Subordinate n=10. Comparison of the sensitivity curves of all three social groups shows that paired-wise interactions had no effect on the response sensitivity (Figure 11B)

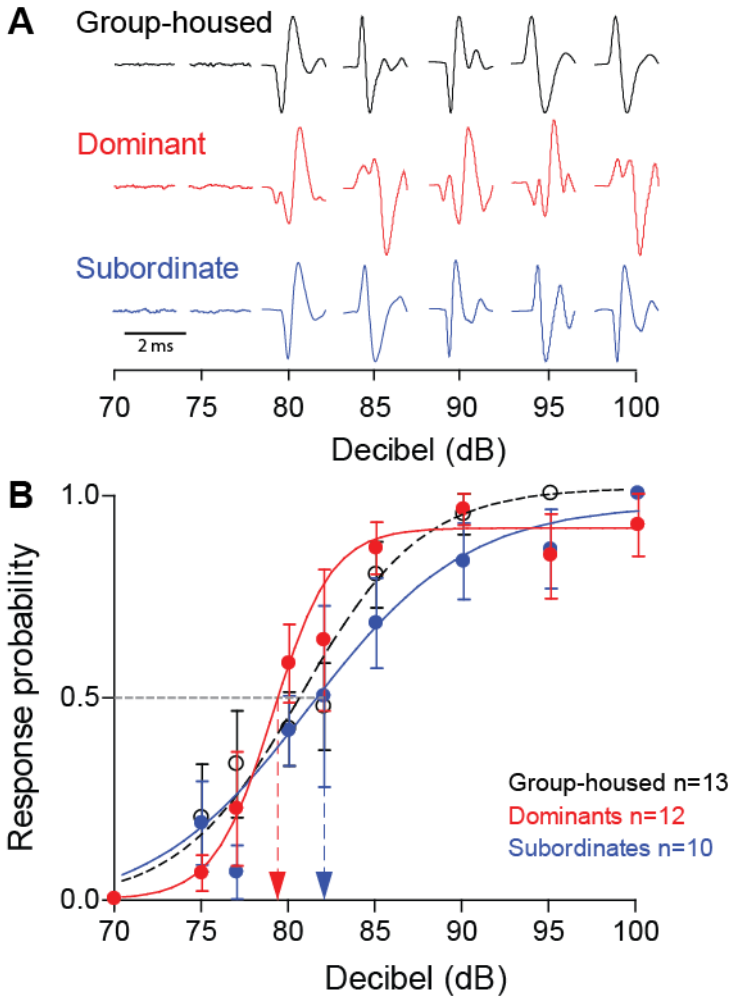

Figure 11 – Lack of visual cues eliminate social rank differences in escape probability
Startle escape response of TLNs is similar in Subordinate, Dominant and group-housed animals. A) Individual examples of c-start field potential from 3 different animals at increasing decibel intensities. B) Probability of initiating an escape response is no higher in Subordinates compared to Dominants and Group-housed at 85-90dB. A response probability of 0.5 is indicated with the dotted line.

DISCUSSION

Our results show that TLN zebrafish, which lack striking skin coloration, show drastically different behavioral choice compared to AB fish. As with AB fish, TLNs show social interactions consisting of primarily one fish attacking and the other fish retreating. In addition, TLN fish do eventually form social hierarchies similar to AB fish, but at a cost to stability of social rank. AB fish showed a negligible presence of the switching of social rank (2/39 pairs observed), while TLN fish showed increased rates of switching (5/16 pairs observed). It is likely that without the ability to display their social rank by way of coloration, TLN zebrafish continue to compete for social dominance during the pairing period whereas their AB counterparts assume their social rank readily. Another stark difference between TLN fish and wild-type fish was in their swimming behavior. By the end of the 2 week pairing period, subordinate AB fish showed a strong preference for the bottom corner of the housing tank, presumably as a form of shelter against the dominant animal (Figure 4B). However, subordinate TLN fish did not display the same place preference, and swam in the same regions of the housing tank occupied by dominant TLN fish (Figure 10B). In addition while Subordinate AB fish showed decreased levels of total swimming activity compared to dominant and group-housed animals, both TLN subordinate and dominant fish showed equal levels of swimming activity; interestingly, these swimming levels by socially experienced TLN fish were greater than that of group-housed animals.

Finally, TLN zebrafish showed no difference in their escape response sensitivities due to social rank (Figure 11B). This was a stark contrast to AB fish, where subordinate fish showed increased sensitivity of their escape circuit (Figure 6B). This again implies that TLN fish are unable to convey their social rank to their counterparts. This lack of visual information from Dominant to Subordinate fish may result in less activation of visually active hypothalamic DA

neurons and therefore reduced modulation of motor outputs like swimming and escape. It also can be noted that the sensitivity of all TLN fish, regardless of rank or social experience, showed increased sensitivity of their M-cell mediated escape compared to AB fish. This may be due to the instability of TLN social hierarchies, and therefore increased stress on both the Dominant and Subordinate animals.

CHAPTER IV

CONCLUSION

The formation of a dominance relationship leads individuals involved to prioritize certain behaviors so that they can adapt to their social climate. In zebrafish, Dominant animals place a priority on swimming so as to assert their dominance. Subordinate zebrafish place a priority on their escape behavior so as to be prepared to be the target of aggression. These behavioral choices are adapted as the dominance relationship forms, and are evidence that social interactions can act as a modulator for behavior. In particular we have found that the DA system is altered by social status, and evidence points to DA being a modulator for both the swimming and escape motor outputs. In addition to DA, visual cues seem to play a pivotal role in regulating behavioral choice. Without the ability to display social rank by the way of visual cues, zebrafish are unable to successfully prioritize adaptive behaviors. This could be either from a lack of stability of dominance relationships, or a breakdown the in neuromodulatory signaling pathways that relies on the processing of visual information between members of a social group. In order to talk more about the interplay between visual information, DA, and social behavior it is necessary to determine how these elements are interconnected within the brain.

In 2011, a comprehensive review was released looking at the conserved neural substrate for social behavior between taxa called the social decision-making network (SDM) [34]. The SDM consist of two components: 1) the social behavior network [47] consists of sex steroid-sensitive regions of the brain, particularly in the hypothalamus, that regulate multiple forms of social behavior like: reproductive behavior, gender-specific sexual behavior, and parental care 2) the mesolimbic reward system containing DA nuclei in the forebrain and hypothalamus that are active during social interactions. O'Connell and Hofmann provide evidence that these two circuits are linked, and that they have an early evolutionary origin in vertebrate species. The

component of the SDN that is of particular interest to this study is the ventral tegmental area (VTA). The VTA is a DA nuclei in the hypothalamus that send projections caudally in the vicinity of both the reticulospinal formation and the nMLF. Therefore the VTA has the propensity to cause DA mediated changes in the escape and swimming outputs of the animal, and is linked to the processing of visual information through the SDM. It is well known that neural circuitry is very complex, and one form of neuromodulation isn't predominant on any one neural circuit. As such, 5-HT and inhibitory signaling by GABA or Glycine may play vital roles into consolidation of and adaptation to social hierarchies in zebrafish; investigation into social status-dependent changes in these signaling pathways would be essential for an improved understanding of the effects of social status on the nervous system. However given the results presented here, the interplay between sensory visual information and DA signaling is an exciting determinant of how animals and people respond to antagonistic social aggressions.

REFERENCES

[1] Ali DW, Drapeau P, Legendre P (2000) Development of Spontaneous Glycinergic Currents in the Mauthner Neuron of the Zebrafish Embryo. J Neurophysiol 85(4):1726-1736

[2] Ampatzis K, Song J, Ausborn J, El Manira A (2013) Pattern of innervation and recruitment of different classes of motoneurons in adult zebrafish. J Neurosci 33:10875-10886

[3] Ampatzis K, Song J, Ausborn J, El Manira A (2014) Separate microcircuit modules of distinct V2a interneurons and motoneurons control the speed of locomotion. Neuron 83(4):934-943

[4] Breder CM, Halpern F (1946) Innate and acquired behavior affecting the aggregation of fishes. Physiological Zoology 19:154-190

[5] Cabelguen JM, Bourcier-Lucas C, Dubuc R (2003) Bimodal locomotion elicited by electrical stimulation of the midbrain in the salamander Notophthalmus viridescens. J Neurosci 23(6):2434-2439

[6] Chang SW, Fagan NA, Toda K, Utevsky AV, Pearson JM, Platt ML (2015) Neural mechanisms of social decision-making in the primate amygdala. Proc Natl Acad Sci USA 112(52):16012-16017

[7] Clements K, Miller T, Ji E, Issa F (2016) The effect of social stress on dopaminergic pathways of the escape circuit of zebrafish. Program No. 442.03. 2016 Society for Neuroscience Meeting Planner. San Diego, CA: Society for Neuroscience, 2016. Online. :

[8] Cuddy AJC, Wilmuth CA, Carney DR (2012) The Benefit of Power Posing Before a High-Stakes Social Evaluation. Harvard Business School Working Paper No. 13-027

[9] Dahlbom JS, Backströmb T, Lundstedt-Enkelc K, Winberg S (2012) Aggression and monoamines: Effects of sex and social rank in zebrafish (Danio rerio). Behav Brain Res 228(2):333-338

[10] Deliagina TG, Zelenin PV, Orlovsky GN (2002) Encoding and decoding of reticulospinal commands. Brain Res Brain Res Rev 40(1-3):166-177

[11] Eaton RC, Farley RD, Kimmel CB, Schabtach E (1977) Functional development in the mauthner cell system of embryos and larvae of the zebra fish. J Neurobiol 8(2):151-172

[12] Eaton RC, Lee RK, Foreman MB (2001) The Mauthner cell and other identified neurons of the brainstem escape network of fish. Prog Neurobiol 62(4):467-485

[13] Ermentrout GB (2002) Simulating, analyzing, and animating dynamical systems: a guide to XPPAUT for researchers and students. SIAM :

[14] Ermentrout GB, Terman DH (2010) Mathematical foundations of neurscience. Springer :

[15] Falkner AL, Lin D (2014) Recent advances in understanding the role of the hypothalamic circuit during aggression. Front Syst Neurosc 8:168

[16] Filby AL, Paull GC, Hickmore TF, Tyler CR (2010) Unravelling the neurophysiological basis of aggression in a fish model. BMC Genomics 11:498

[17] Giacomini AC, Abreu MS, Giacomini LV, Siebel AM, Zimerman FF, Rambo CL, Mocelin R, Bonan CD, Piato AL, Barcellos LJ (2015) Fluoxetine and diazepam acutely modulate stress induced-behavior. Behav Brain Res 296:301-310

[18] Hatamoto K, Shingyoji C (2008) Cyclical training enhances the melanophore responses of zebrafish to background colours. Pigment Cell Melanoma Res 21:397-406

[19] Hatta K, Korn H (1998) Physiological Properties of the Mauthner System in the Adult Zebrafish. J Comp Neurol 365(4):492-509

[20] Höglund E, Balm PHM, Winberg S (2000) Skin darkening, a potential social signal in subordinate artic charr (salvelinus alpinus): The regulatory role of brain monoamines and pro-opiomelanocortin-derived peptides. J Exp Biol 203:1711-1721

[21] Höjesjö J, Axelsson M, Dahy R, Gustavsson L, Johnsson JI (2015) Sight or smell - Behavioral and heart rate response in subordinate rainbow trout exposed to cues from dominant fish. PeerJ 3:e1169

[22] Huntingford FA, Turner AK (1987) Animal Conflict. London: Chapman & Hall

[23] Issa FA, Drummond J, Cattaert D, Edwards DH (2012) Neural circuit reconfiguration by social status. J Neurosci 32(16):5638-5645

[24] Izhikevich EM (2007) Dynamical systems in neuroscience: The geometry of excitability and bursting. MIT Press

[25] Johnsson, JI (1997) Individual Recognition Affects Agression and Dominance Relations in Rainbow Trout (Oncorhynchus mykiss). Ethology 104(4):267-282

[26] Jones SR, Gainetdinov RR, Jaber M, Giros B, Wightman RM, Caron MG (1998) Profound neuronal plasticity in response to inactivation of the dopamine transporter. Proc Natl Acad Sci USA 95(7):4029-34

[27] Kashin SM, Feldman AG, Orlovsky GN (1974) Locomotion of fish evoked by electrical stimulation of the brain. Brain Res 82(1):41-47

[28] Koblinger K , Fuzesi T , Ejdrygiewicz J, Krajacic A, Bains JS, Whelan PJ (2014) Characterization of A11 Neurons Projecting to the Spinal Cord of Mice. PLoS One 9(10):e109636

[29] Kohashi T, Oda Y (2008) Initiation of Mauthner- or non-Mauthner-mediated fast escape evoked by different modes of sensory input. J Neurosci 28(42):10641-10653

[30] Korn H, Faber DS (2005) The Mauthner cell half a century later: a neurobiological model for decision-making?. Neuron 47:13-28

[31] Korzan WJ, Robison RR, Zhao S, Fernald RD (2008) Color change as a potential behavioral strategy. Horm Behav 54(3):463-470

[32] Krug, E, Dahlberg L, Mercy J, Zwi A, Lozano R (2002) World report on violence and health. Biomedica 22 Suppl 2:327-336

[33] Lacoste AM, Schoppik D, Robson DN, Haesemeyer M, Portugues R, Li JM, Randlett O, Wee CL, Engert F, Schier AF (2015) A convergent and essential interneuron pathway for mauthner-cell-mediated-escapes. Curr Biol 25(11):1526-1534

[34] Lambert AM, Bonkowsky JL, Masino MA (2012) The Conserved Dopaminergic Diencephalospinal Tract Mediates Vertebrate Locomotor Development in Zebrafish Larvae. J Neurosci 32(39):13488-13500

[35] Larson ET, O'Malley DM, Melloni RH Jr (2006) Aggression and vasotocin are associated with dominant–subordinate relationships in zebrafish. Behav Brain Res 167:94-102

[36] Lister JA, Robertson CP, Lepage T, Johnson SL, Raible DW (1999) nacre encodes a zebrafish microphthalmia-related protein that regulates neural-crest-derived pigment cate fate. Development 126:3757-3767

[37] Logan DW, Burn SF, Jackson IJ (2006) Regulation of pigmentation in zebrafish melanophores. Pigment Cell Res 19:206-213

[38] Mansur BM, Dos Santos BR, Dias Ca, Pinheiro MS, Gouveia A (2014) Effects of the number of subjects on the dark/light preference of zebrafish (Danio rerio). Zebrafish 11(6):560-566

[39] Manuel R, Gorissen M, Zethof J, Ebbesson LO, van de Vis H, Flik G, van den Bos R (2014) Unpredictable chronic stress decreases inhibitory avoidance learning in Tuebingen long-fin zebrafish: stronger effects in the resting phase than in the active phase. J Exp Biol 217(21):3919-3928

[40] McCann LI, Koehn DJ, Kline KJ (1971) The effects of body size and body marking on nonpolarized schooling behavior of zebrafish (Brachydanio rerio). J Psych 79:71-75

[41] McLean DL, Fetcho JR (2004) Relationship of tyrosine hydroxylase and serotonin immunoreactivity to sensorimotor circuitry in larval zebrafish. J Comp Neurol 480(1):57-71

[42] Medan V, Preuss T (2014) The Mauthner-cell circuit of fish as a model system for startle plasticity. J Physiol Paris 108(2-3):129-140

[43] Mizrahi, R (2015) Social Stress and Psychosis Risk: Common Neurochemical Substrates?. Neuropsychopharmacology 41(3):666-674

[44] Morris C, Lecar H (1981) Voltage oscillations in the barnacle giant muscle fiber. J Physiol Paris 108(2-3):129-140

[45] Mu Y, Li XQ, Zhang B, Du JL (2012) Visual input modulates audiomotor function via hypothalamic dopaminergic neurons through a cooperative mechanism. Neuron 75(4):688-699

[46] Neumeister H, Whitaker KW, Hofmann HA, Preuss T (2010) Social and ecological regulation of a decision-making circuit. J Neurophysiol 104(6):3180-3188

[47] Newman SW (1999) The medial extended amygdala in male reproductive behavior. A node in the mammalian social behavior network. Ann N Y Acad Sci 877:242-257

[48] O'Connell L, Hofmann H (2011) The Vertebrate Mesolimbic Reward System and Social Behavior Network: A Comparative Synthesis. J Comp Neurol 519:3599-3639

[49] Oda Y,Kawasaki K, Morita M, Korn H, Matsui H (1998) Inhibitory long-term potentiation underlies auditory conditioning of goldfish escape behaviour. Nature 394(6689):182-185

[50] Oliveira RF, Silva FJ, Simões JM (2011) Fighting zebrafish: characterization of aggressive behavior and winner-loser effects. Zebrafish 8(2):73-81

[51] O'Malley DM, Kao YH, Fetcho JR (1996) Imaging the functional organization of zebrafish hindbrain segments during escape behaviors. Neuron 17(6):1145-1155

[52] Paull GC, Filby AL, Giddins HG, Coe TS, Hamilton PB, Tyler CR (2010) Dominance hierarchies in zebrafish (Danio rerio) and their relationship with reproductive success. Zebrafish 7:109-117

[53] Pavlidis M, Sundvik M, Chen YC, Panula P (2011) Adaptive changes in zebrafish brain in dominant-subordinate behavioral context. Behav Brain Res 225(2):529-537

[54] Pavlik LL, Bezgina EN, Tiras NR, Mikheeva IB, Udal'tsov SN, Moshkov DA (2005) The Structure of Mixed Synapses in Mauthner Neurons During Exposure to Substances Altering Gap Junction Conductivity. Neurosci Behav Physiol 35(5):447-452

[55] Pereda A, Triller A, Korn H, Faber DS (1992) Dopamine enhances both electrotonic coupling and chemical excitatory postsynaptic potentials at mixed synapses. Proc Natl Acad Sci USA 89(24):12088-12092

[56] Pereda AE, Nairn AC, Wolszon LR, Faber DS (1994) Postsynaptic Modulation of Synaptic Efficacy at Mixed Synapses on the Mauthner Cell. J Neurosci 14(6):3704-3712

[57] Platt ML, Seyfarth RM, Cheney DL (2016) Adaptations for social cognition in the primate brain. . Philos Trans R Soc Lond B Biol Sci 371(1687):20150096

[58] Preuss T, Faber DS (2003) Central cellular mechanisms underlying temperature-dependent changes in the goldfish startle-escape behavior. J Neurosci 23(13):5617-5626

[59] Prugh JI, Kimmel CB, Metcalfe WK (1982) Noninvasive recording of the Mauthner neuron action potential in larval zebrafish. J Exp Biol 101:83-92

[60] Pyron M (2003) Female preferences and male-male interactions in zebrafish (Danio rerio). Can J Zool 81:122-125

[61] Rodriguiz RM, Chu R, Caron MG, Westel WC (2004) Aberrant responses in social interaction of dopamine transporter knockout mice. Behav Brain Res 148(1-2):185-189

[62] Romanov K, Appelberg K, Honkasalo ML, Koskenvuo M (1996) Recent interpersonal conflict at work and psychiatric morbidity: a prospective study of 15,530 employees aged 24-64. Journal of Psychosomatic Research 40(2):169-176

[63] Roy B, Ferdous J, Ali DW (2015) NMDA Receptors on Zebrafish Mauthner Cells Require CaMKII-alpha for Normal Development. Dev Neurobiol 75(2):145-162

[64] Sankrithi NS, O'Malley DM (2010) Activation of a Multisensory, Multifunctional Nucleus in the Zebrafish Midbrain during Diverse Locomotor Behaviors. J Neuro 166:970-993

[65] Sato T, Hamaoka T, Aizawa H, Hosoya T, Okamoto H (2007) Genetic single-cell mosaic analysis implicates ephrinB2 reverse signaling in projections from the posterior tectum to the hindbrain in zebrafish. J Neurosci 27(20):5271-5279

[66] Severi KE, Portugues R, Marques JC, O'Malley DM, Orger MB, Engert F (2014) Neural control and modulation of swimming speed in the larval zebrafish. Neuron 83(3):692-707

[67] Song J, Ampatzis K, Ausborn J, El Manira A (2015) A hardwired circuit supplemented with endocannabinoids encodes behavioral choice in zebrafish. Curr Bio 25:2610-2620

[68] Thiele TR, Donovan JC, Baier H (2014) Descending control of swim posture by a midbrain nucleus in zebrafish. Neuron 83(3):679-691

[69] Venables WN, Ripley BD (2002) Modern Applied Statistics with S. Fourth Edition. Springer, New York. ISBN 0-387-95457-0

[70] Wang WC, McLean DL (2014) Selective responses to tonic descending commands by temporal summation in a spinal motor pool. Neuron 83(3):708-721

[71] Whitaker KW, Neumeister H, Huffman LS, Kidd CE, Preuss T, Hofmann HA (2011) Serotonergic modulation of startle-escape plasticity in an African cichlid fish: a single-cell molecular and physiological analysis of a vital neural circuit. J Neurophysiol 106(1):127-137

[72] Wilson EO (1975) Sociobiology. Cambridge, MA: Harvard University Press

[73] Yamaguchi Y, Lee YA, Kato A, Goto Y (2016) The Roles of Dopamine D1 Receptor on the Social Hierarchy of Rodents and Nonhuman Primates. Int J Neuropsychopharmacol pyw106

[74] Yamamoto K, Vernier P (2011) The evolution of dopamine systems in chordates. Front Neuroanat 5:21

[75] Yao C, Vanderpool KG, Delfiner M, Eddy V, Lucaci AG, Soto-Riveros C, Yasumura T, Rash JE, Pereda AE (2014) Electrical synaptic transmission in developing zebrafish: properties and molecular composition of gap junctions at a central auditory synapse. J Neurophysiol 112(9):2102-2113

[76] Yao Y, Li X, Zhang B, Yin C, Liu Y, Chen W, Zeng S, Du J (2016) Visual Cue-Discriminative Dopaminergic Control of Visuomotor Transformation and Behavior Selection. Neuron 89(3):598-612

[77] Yeh SR, Fricke RA, Edwards DH (1996) The effect of social experience on serotonergic modulation of the escape circuit of crayfish. Science 271:366 –369

[78] Zottoli SJ (1977) Correlation of the startle reflex and Mauthner cell auditory responses in unrestrained goldfish. J Exp Biol 66:243-254

[79] Zottoli SJ, Faber DS (2000) The Mauthner cell: what has it taught us?. Neuroscientist 6:26-38

[80] Zottoli SJ, Marek LE, Agostini MA, Strittmatter SL (1987) Morphological and physiological survival of goldfish Mauthner axons isolated from their somata by spinal-cord crush. J Comp Neurol 255:272–282

APPENDIX: IACUC APPROVAL LETTERS

East Carolina University

Animal Care and Use Commitee
212 Ed Warren Life Sciences Building
East Carolina University
Greenville, NC 27834

252-744-2436 office
252-744-2355 fax

December 1, 2014

Fadi Issa, Ph.D.
Department of Biology
Howell Science Complex
East Carolina University

Dear Dr. Issa:

Your Animal Use Protocol entitled, "Developmental and Functional Effects of Spinocerebellar Ataxia Type-13 on Zebrafish Cerebellum and the Effects of Social Experience on Zebrafish Startle Escape Response" (AUP #D320) was reviewed by this institution's Animal Care and Use Committee on 12/1/14. The following action was taken by the Committee:

"Approved as submitted"

Please contact Dale Aycock at 744-2997 prior to hazard use

A copy is enclosed for your laboratory files. Please be reminded that all animal procedures must be conducted as described in the approved Animal Use Protocol. Modifications of these procedures cannot be performed without prior approval of the ACUC. The Animal Welfare Act and Public Health Service Guidelines require the ACUC to suspend activities not in accordance with approved procedures and report such activities to the responsible University Official (Vice Chancellor for Health Sciences or Vice Chancellor for Academic Affairs) and appropriate federal Agencies. **Please ensure that all personnel associated with this protocol have access to this approved copy of the AUP and are familiar with its contents.**

Sincerely yours,

Susan McRae, Ph.D.
Chair, Animal Care and Use Committee

SM/jd

Enclosure

East Carolina University

Animal Care and Use Commitee
212 Ed Warren Life Sciences Building
East Carolina University
Greenville, NC 27834

252-744-2436 office
252-744-2355 fax

MEMORANDUM

TO: Thomas Miller
Department of Biology

FROM: Dorcas O'Rourke, D.V.M.
University Veterinarian

SUBJECT: Certificate of Training
Training Date 12/2/15

DATE: December 2, 2015

This letter is provided to certify that you have completed training in humane methods of animal experimentation, proper handling of selected species of research animals, and methods for reporting deficiencies in animal care and treatment. The training was provided in accordance with U.S. Department of Agriculture (9 CFR 2.32) regulations and the Public Health Service Policy.

This training included information on ECU animal care organizational structure, regulatory requirements, IACUC procedures, program for veterinary and animal care, occupational health and safety program, and methods for reporting concerns. Information on biology and care, proper restraint and procedures, and allergies and zoonoses were also provided.

We suggest that you retain this letter in your training file for future reference.